Food and Chemical Toxicology 133 (2019) 110794

Contents lists available at ScienceDirect

Food and Chemical Toxicology

journal homepage: www.elsevier.com/locate/foodchemtox

Toxic essential oils, part VI: Acute oral toxicity of lemon balm (*Melissa officinalis* L.) essential oil in BALB/c mice

Nikola M. Stojanović[a,**], Pavle J. Randjelović[b], Marko Z. Mladenović[c], Ivan R. Ilić[d], Vladimir Petrović[e], Nenad Stojiljković[b], Sonja Ilić[b], Niko S. Radulović[c,*]

[a] Faculty of Medicine, University of Niš, Zorana Đinđića 81, 18000, Niš, Serbia
[b] Department of Physiology, Faculty of Medicine, University of Niš, Zorana Đinđića 81, 18000, Niš, Serbia
[c] Department of Chemistry, Faculty of Sciences and Mathematics, University of Niš, Višegradska 33, 18000, Niš, Serbia
[d] Institute of Pathology, Faculty of Medicine, University of Niš, Zorana Đinđića 81, 18000, Niš, Serbia
[e] Department of Histology and Embryology, Faculty of Medicine, University of Niš, Zorana Đinđića 81, 18000, Niš, Serbia

ARTICLE INFO

Keywords:
Melissa officinalis L. (Lamiaceae)
Essential oil
Oral toxicity in mice
Biochemical parameters
Histopathological changes
Behavioral alterations

ABSTRACT

Despite being renowned for its volatiles, the data on the toxicity of the essential oil of lemon balm (*Melissa officinalis* L., Lamiaceae) is rather limited compared to its solvent/water-soluble extractibles. In this study, the aerial parts essential oil of *M. officinalis*, with over 130 constituents identified herein, 26 of which detected for the first time, was investigated for acute oral toxicity in BALB/c mice. The oil, composed of predominantly monoterpene aldehydes, citronellal (21.2–21.8%), neral (17.8–18.4%), and geranial (22.9–23.5%), which were assayed in parallel with the oil in some tests, induced significant changes in animal behavior, as well as altered biochemical parameters reflecting liver and kidney functions. Different pathological changes in the stomach, duodenum, liver, and kidneys were detected when the oil was administered in doses higher than 1 g kg^{-1}. A depletion in the liver/kidney antioxidant capacities and an increased rate of lipid peroxidation was noted for animals treated with lemon balm oil. The calculated value of the oral LD_{50} in BALB/c mice (2.57 g kg^{-1}) infers that the essential oil is only moderately toxic.

1. Introduction

The common belief that all herbal remedies and related natural-based products are only beneficial, and completely safe to use, could cause devastating consequences to consumers' health (Radulović et al., 2013a). The most frequently applied form of plant preparations, i.e. extracts, are obtained through specific physicochemical processes (solvent extraction, (hydro)distillation, pressing, etc.). Lemon balm (*Melissa officinalis* L., Lamiaceae) is a widely distributed plant species throughout Europe and is valued in the traditional medicines of Balkan peoples due to its sedative, antispasmodic, digestive, antibacterial, antiviral, and antifungal properties (Ulbricht et al., 2005). Besides the mentioned activities, *M. officinalis* is claimed to possess numerous other beneficial properties, but that lack sufficient scientific evidence, which include the treatment of serious gastrointestinal, cardiovascular and central nervous system (CNS) disorders, as well as malignancies (Ulbricht et al., 2005). Sometimes, it is even proposed to be an herbal cure-all (Ulbricht et al., 2005). Commercially available dry extracts of *M. officinalis* or other herbal products containing this taxon together with other species are documented to be utilized by psychiatric patients suffering from anxiety and depressive disorders, as well as from insomnia (Stojanović et al., 2017).

It is not clear what are the optimal doses of *M. officinalis* extracts needed to exert the full desired (potential) effect and to be at the same time safe to use. *Melissa officinalis* has been placed on the FDA list and is generally regarded as safe (GRAS list) (Ulbricht et al., 2005), i.e. safe when orally consumed in usual amounts found in food-stuff for up to 30 days. However, theoretically, it is unsafe for use during pregnancy or lactation, in the pediatric population or in patients suffering from thyroid disorders or in combination with sedatives (Ulbricht et al., 2005). It is commercially available in most EU member countries in different formulations (drops, capsules, tablets, etc.) (Barnes et al., 2002). *Melissa officinalis folium* is used as a fragrance for wine, tea, and beer and is listed by the Council of Europe as a natural food flavoring agent in the category N2, indicating that lemon balm can be added to foodstuffs in small quantities (Barnes et al., 2002). Several clinical trials

* Corresponding author.
** Corresponding author.
E-mail addresses: nikola.st90@yahoo.com (N.M. Stojanović), nikoradulovic@yahoo.com (N.S. Radulović).

https://doi.org/10.1016/j.fct.2019.110794
Received 4 August 2019; Received in revised form 23 August 2019; Accepted 24 August 2019
Available online 29 August 2019
0278-6915/

reported contradictory findings on the occurrence of adverse effects that follow *M. officinalis* usage. There are claims that when consumed orally, *M. officinalis* is well tolerated for up to 8 weeks of application. A case is reported of an occurrence of headache, changes in EEG, reduction of alertness and tiredness that followed the application of a single dose of *M. officinalis* extract (Ulbricht et al., 2005).

The amount of essential oil in dry *M. officinalis* herb is believed to be ranging from 0.08 to 0.25 mL/100 g (Patora et al., 2003). The essential oils' major constituents include monoterpenes, citronellal, geranial, neral, methyl citronellate, ocimene, citronellol, geraniol, and linalool, and sesquiterpenes, such as β-caryophyllene and germacrene D. Most frequently, citronellal, geranial, and neral constitute about 50–70% of the oil (Ulbricht et al., 2005). The essential oil found its application in Germany for the treatment of insomnia and headaches (Ulbricht et al., 2005), whereas in Austria it is used to alleviate gastrointestinal, nervous, hepatic and biliary ailments (Vogl et al., 2013). On the Balkan Peninsula, in the Republic of Macedonia, the oil is used for the treatment of heart conditions and headaches (Shakeri et al., 2016). Additionally, there are studies that evaluated the anti-agitation activity of the oil in people suffering from severe dementia, where the oil treatment produced a statistically significant decrease in agitation (Ballard et al., 2002). Both the ethnopharmacological utilization of lemon balm and the one that found its place in official pharmacopeias are frequently connected, in addition to the non-volatile phenolic compounds, to the content of the essential oil present in the herbal material (Ulbricht et al., 2005).

Our previous investigations involved the toxicological evaluation of different essential oils, as well as pure essential-oil constituents (Radulović et al., 2012; 2013a; 2013b; 2015a; 2015b; 2017), using a variety of both *in vitro* and in vivo experimental models. Prompted by lemon balm (*M. officinalis*) traditional usage for the treatment of different psychiatric disorders (Stojanović et al., 2017), among numerous other beneficial properties, and the lack of data on the general safety of its essential oil, in this work we aimed to assess the toxicological properties of the mentioned essential oil. Since *M. officinalis* essential oil is one of the main bioactive principles of the plant species, we decided, prior to in vivo experiments, to investigate its *in vitro* cytotoxicity on primary mouse immune system cells (macrophages and lymphocytes) and the acute toxicity in the *Artemia salina* model. Following the application of the oil in high doses, we observed its influence on the general behavior of the treated mice. In addition to that, serum/tissue biochemical parameters and tissue microscopic examination, reflecting the liver, kidney and gastrointestinal tract function/states, were performed.

2. Materials and methods

2.1. Drugs and chemicals

All solvents (HPLC grade) were purchased from Sigma-Aldrich (St. Louis, Missouri, USA). A mixture of both stereoisomers of citral (59.8% of (*E*)-citral (geranial) and 40.2% of (*Z*)-citral (neral), based on quantitative ^{1}H NMR), and pure citronellal were purchased from Sigma-Aldrich (St. Louis, Missouri, USA). Streptomycin, penicillin G, and 3-(4,5-dimethylthiazol-2-yl)-2,5-diphenyltetrazolium bromide (MTT) were purchased from AppliChem (Darmstadt, Germany), while dexamethasone (Dex) was acquired from Galenika (Beograd, Serbia). The cell medium (RPMI, acquired from Sigma-Aldrich, USA) used in *in vitro* experiments consisted of RPMI 1640 with 20 mM HEPES and L-glutamine, without sodium bicarbonate, containing 5% of fetal bovine serum, 200 mg mL^{-1} streptomycin and 200 IU mL^{-1} penicillin.

2.2. Plant material

Plant material, originating from a single, wild-growing *Melissa officinalis* L. (Lamiaceae) population (sample **MO-1**), was collected at the beginning of July 2015, in the village Veliki Drenovac (near the city of Niš, Serbia, 280 m above sea level, 43°24′21″N and 21°44′21″E). One of the authors (N.S.R.) performed the botanical identification of the plant material during collection. Voucher specimens were deposited in the Herbarium of the Faculty of Sciences and Mathematics, University of Niš, Serbia under the accession number NR-0913, where a trained botanist, the custodian of the mentioned herbarium, confirmed their identity.

2.3. Essential-oil extraction

Fresh aerial parts were, immediately after collection, submitted to hydrodistillation for 2.5 h, using the original Clevenger-type apparatus (Radulović et al., 2015a). The obtained oil (sample **MO-1**) was separated by extraction with diethyl ether, dried over anhydrous magnesium sulfate and immediately analyzed by GC-MS. The hydrodistillation of the aerial parts yielded 0.09% (*w/w*) of a yellowish, fragrant essential oil. The essential-oil sample **MO-2** was purchased from a local herb shop in Niš (produced by Siempreviva, Niš, Serbia).

2.4. Gas chromatography-mass spectrometry (GC-MS) analyses

The GC-MS analyses (three repetitions) were carried out using a Hewlett-Packard 6890N gas chromatograph equipped with a fused silica capillary column DB-5MS (5% phenylmethylsiloxane, 30 m × 0.25 mm, film thickness 0.25 μm, Agilent Technologies, USA) and coupled with a 5975B mass selective detector from the same company. The injector and interface were operated at 250 °C and 300 °C, respectively. Oven temperature was raised from 70 to 290 °C at a heating rate of 5 °C min^{-1}; the heating program ended with an isothermal period of 10 min. As a carrier gas helium at 1.0 mL min^{-1} was used. The samples (10 mg of *M. officinalis* essential oil was dissolved in 1 mL of Et_2O) were injected in a pulsed split mode (injection volume was 1 μL; the flow was 1.5 mL min^{-1} for the first 0.5 min and then set to 1.0 mL min^{-1} throughout the remainder of the analysis; split ratio 40 : 1). MS conditions were as follows: ionization voltage of 70 eV, acquisition mass range 35–650, scan time 0.32 s. The essential oil samples and authentic standards (wherever possible) were also analyzed by GC-MS using an HP-Innowax FSC polyethylene glycol polar column (60 m × 0.25 mm, film thickness 0.25 mm; Agilent Technologies, Santa Clara, CA, USA). Initial oven temperature was 60 °C for 10 min and increased at 4 °C min^{-1} to 220 °C, then kept constant at 220 °C for 10 min and increased at 1 °C min^{-1} to 240 °C. All other GC-MS analysis and instrument parameters were as described above.

2.5. Gas chromatography-flame ionization detector (GC-FID) analyses

The GC-FID analyses were carried out using an Agilent 7890A GC system equipped with a single injector, one flame ionization detector (FID) and a fused silica capillary column HP-5MS (5% phenylmethylsiloxane, 30 m × 0.32 mm, film thickness 0.25 μm, Agilent Technologies, USA). The oven temperature was programmed from 70 °C to 300 °C at 15 °C min^{-1} and then held isothermally at 300 °C for 5 min; the carrier gas was nitrogen at 3.0 mL min^{-1}; the injector temperature was held at 250 °C. The samples, 1.0 μL of the corresponding solutions, were injected in a splitless mode. The parameters of the FID detector were as follows: heater temperature–300 °C, H_2 flow–30 mL min^{-1}, air flow–400 mL min^{-1}, makeup flow–23.5 mL min^{-1}, data collection–Agilent GC ChemStation with a digitization rate of 20 Hz.

2.6. Component identification

Essential-oil constituents were identified by comparison of their linear retention indices (relative to C_7–C_{33} alkanes (Van den Dool and Kratz, 1963) on DB-5MS and HP-Innowax column) with literature values (Table S1) and their mass spectra with those of authentic

Table 1
The chemical composition of the two samples of the essential oil of *M. officinalis*.

RI_{exp}[a]	RI_{lit}[b]	Compound	Class[c]	Percentage (%)[d]		Identification[e]
				MO-1	MO-2	
778	778	3-Methyl-2-butenal	FAD	tr	/	RI, MS
800	800	Octane[f,g]	FAD	/	tr	RI, MS, Co-GC
801	801	Hexanal	FAD	tr	tr	RI, MS, Co-GC
842	844	(*E*)-3-Hexen-1-ol	FAD	tr	/	RI, MS
849	850	(*Z*)-3-Hexen-1-ol	FAD	0.2	0.2	RI, MS
856	859	(*Z*)-2-Hexen-1-ol	FAD	0.2	tr	RI, MS
861	863	1-Hexanol	FAD	/	tr	RI, MS, Co-GC
885	885	2-Butylfuran[f]	FAD	tr	tr	RI, MS
915	913	(*Z*)-3-Hexenyl formate[f]	FAD	tr	/	RI, MS
935	932	α-Pinene	MH	/	tr	RI, MS, Co-GC
948	945	4,4-Dimethyl-2-buten-4-olide[f]	O	tr	/	RI, MS
953	946	Camphene	MH	/	tr	RI, MS, Co-GC
960	952	Benzaldehyde	O	tr	tr	RI, MS, Co-GC
975	974	1-Octen-3-ol	FAD	0.5	0.4	RI, MS
981	979	6-Methyl-5-hepten-2-one	MO	2.9	2.0	RI, MS
981	979	3-Octanone	FAD	tr	/	RI, MS
987	988	Myrcene	MH	0.2	tr	RI, MS, Co-GC
989	984	2-Pentylfuran	FAD	/	tr	RI, MS
993	988	Dehydro-1,8-cineole	MO	tr	tr	RI, MS
995	993	3-Octanol	FAD	tr	tr	RI, MS
1002	1004	(*E*)-3-Hexenyl acetate[f]	FAD	0.2	0.1	RI, MS
1008	1007	Hexyl acetate	FAD	/	tr	RI, MS, Co-GC
1010	1010	(*E*)-2-Hexenyl acetate	FAD	/	tr	RI, MS
1026	1020	*p*-Cymene	MH	tr	tr	RI, MS
1031	1024	Limonene	MH	0.1	tr	RI, MS
1033	1026	1,8-Cineole	MO	0.2	tr	RI, MS, Co-GC
1044	1044	(*E*)-β-Ocimene	MH	0.3	0.3	RI, MS
1051	1044	2,6-Dimethyl-5-heptenal	MO	0.2	0.1	RI, MS
1057	1039	3-Methyl-2-cyclohexen-1-one[f]	MO	tr	/	RI, MS
1067	1063	1-Octanol	FAD	tr	/	RI, MS, Co-GC
1070	1067	*cis*-Linalool oxide (furanoid)	MO	/	tr	RI, MS
1071	1065	*cis*-Sabinene hydrate	MO	tr	tr	RI, MS
1078	1072	*m*-Cresol[f]	O	tr	/	RI, MS, Co-GC
1092	1091	Rose furan	MO	tr	tr	RI, MS
1094	1091	1-Undecene[f]	FAD	tr	/	RI, MS
1100	1098	Linalool	MO	1.9	1.4	RI, MS, Co-GC
1104	1100	Nonanal	FAD	0.3	0.3	RI, MS, Co-GC
1111	1106	*cis*-Rose oxide	MO	0.6	0.5	RI, MS
1121	1123	Methyl octanoate[f]	FAD	tr	/	RI, MS, Co-GC
1127	1122	*trans*-Rose oxide	MO	0.4	0.2	RI, MS
1138	1123	*cis*,*cis*-Photocitral A	MO	tr	0.1	RI, MS
1144	1147	*exo*-Isocitral	MO	0.8	0.3	RI, MS
1146	1140	*cis*-β-Terpineol	MO	tr	/	RI, MS
1152	1148	Citronellal	MO	21.2	21.8	RI, MS, Co-GC
1157	1148	*trans*-*p*-Menthan-3-one	MO	tr	tr	RI, MS
1160	1160	(*Z*)-Isocitral	MO	0.4	0.4	RI, MS
1162	1155	*iso*-Isopulegol	MO	0.8	0.5	RI, MS
1163	1165	Lavandulol	MO	/	tr	RI, MS
1166	1158	*cis*-*p*-Menthan-3-one	MO	tr	tr	RI, MS
1169	1173	Rosefuran epoxide	MO	tr	tr	RI, MS
1170	1165	1-Nonanol	FAD	/	tr	RI, MS, Co-GC
1172	1167	*neoiso*-Isopulegol	MO	/	tr	RI, MS
1173	1172	*p*-Mentha-1,5-dien-8-ol	MO	tr	tr	RI, MS
1174	1176	Borneol	MO	/	tr	RI, MS, Co-GC
1177	1177	Isopulegone	MO	tr	tr	RI, MS, Co-GC
1179	1177	(*E*)-Isocitral	MO	0.9	1.3	RI, MS
1184	1183	Terpinen-4-ol	MO	0.5	0.4	RI, MS, Co-GC
1185	1187	*trans*-*p*-Mentha-1(7),8-dien-2-ol	MO	tr	/	RI, MS
1187	1187	*p*-Cymen-8-ol	MO	tr	tr	RI, MS
1191	1191	Hexyl butanoate	FAD	/	tr	RI, MS
1197	1186	α-Terpineol	MO	tr	tr	RI, MS
1206	1201	Decanal	FAD	/	tr	RI, MS, Co-GC
1212	1204	Verbenone	MO	tr	tr	RI, MS
1225	1223	Citronellol	MO	2.1	2.6	RI, MS, Co-GC
1229	1227	Nerol	MO	tr	tr	RI, MS, Co-GC
1233	1233	Hexyl 2-methylbutanoate	FAD	tr	tr	RI, MS, Co-GC
1236	1227	Neral	MO	18.4	17.8	RI, MS, Co-GC
1250	1254	Linalyl acetate	MO	1.8	1.5	RI, MS
1252	1249	Geraniol	MO	1.2	1.6	RI, MS, Co-GC

(*continued on next page*)

Table 1 (*continued*)

RI_{exp}[a]	RI_{lit}[b]	Compound	Class[c]	Percentage (%)[d]		Identification[e]
				MO-1	MO-2	
1258	1257	Methyl citronellate	MO	2.8	2.3	RI, MS
1258	1249	Piperitone	MO	tr	tr	RI, MS
1262	1260	(*E*)-2-Decenal[f]	FAD	/	tr	RI, MS
1266	1264	Geranial	MO	22.9	23.5	RI, MS, Co-GC
1272	1271	Citronellyl formate	MO	/	tr	RI, MS
1276	1280	Neryl formate	MO	tr	tr	RI, MS
1283	1288	Lavandulyl acetate	MO	0.5	0.5	RI, MS
1283	1252*	*trans*-7-Hydroxy-3,7-dimethyl-3,6-oxyoctanal[f]	MO	tr	tr	RI, MS
1286	1257*	*cis*-7-Hydroxy-3,7-dimethyl-3,6-oxyoctanal[f]	MO	tr	tr	RI, MS
1298	1298	Geranyl formate	MO	tr	tr	RI, MS, Co-GC
1306	1305	Undecanal[f]	FAD	tr	tr	RI, MS, Co-GC
1315	1312	Citronellic acid	MO	0.6	0.5	RI, MS, Co-GC
1321	1322	Methyl geranate	MO	0.9	1.1	RI, MS, Co-GC
1324	1340	Neric acid	MO	tr	/	RI, MS, Co-GC
1327	1330	Hexyl tiglate	FAD	tr	tr	RI, MS, Co-GC
1335	1302*	6,7-Epoxyneral[f]	MO	tr	tr	RI, MS
1340	1328	(1*R**,3*S**,4*R**)-p-Menthan-3,8-diol[f]	MO	/	tr	RI, MS, Co-GC
1341	1340	Piperitenone	MO	tr	/	RI, MS, Co-GC
1351	1337*	6,7-Epoxygeranial[f]	MO	tr	0.3	RI, MS
1352	1350	Citronellyl acetate	MO	tr	tr	RI, MS, Co-GC
1357	1359	Neryl acetate	MO	0.2	0.2	RI, MS, Co-GC
1365	1359	Geranic acid	MO	tr	tr	RI, MS, Co-GC
1366	/	(1*R**,3*R**,4*R**)-*p*-Menthan-3,8-diol[f]	MO	tr	tr	MS, Co-GC
1377	1379	Geranyl acetate	MO	3.1	3.0	RI, MS, Co-GC
1379	1374	α-Copaene	SH	tr	tr	RI, MS
1384	1382	Hexyl hexanoate	FAD	/	tr	RI, MS, Co-GC
1387	1387	β-Bourbonene	SH	tr	tr	RI, MS
1390	1387	β-Cubebene	SH	tr	tr	RI, MS
1392	1389	β-Elemene	SH	tr	/	RI, MS
1400	1400	Tetradecane	FAD	tr	tr	RI, MS, Co-GC
1408	1408	(*Z*)-Caryophyllene	SH	/	tr	RI, MS
1423	1417	(*E*)-Caryophyllene	SH	7.9	9.2	RI, MS, Co-GC
1435	1432	*trans*-α-Bergamotene	SH	/	tr	RI, MS
1452	1454	(*E*)-β-Farnesene	SH	tr	tr	RI, MS
1458	1452	α-Humulene	SH	0.4	0.6	RI, MS
1460	1461	2-Methyltetradecane[f]	FAD	/	tr	RI, MS
1463	1464	*allo*-Aromadendrene	SH	tr	tr	RI, MS
1464	1464	9-*epi*-(*E*)-Caryophyllene	SH	tr	/	RI, MS
1483	1484	Germacrene D	SH	tr	0.2	RI, MS, Co-GC
1489	1483	(*E*,*Z*)-α-Farnesene	SH	tr	tr	RI, MS
1498	1493	*epi*-Cubebol[f]	SO	tr	/	RI, MS
1500	1500	α-Muurolene	SH	tr	tr	RI, MS
1503	1505	(*E*,*E*)-α-Farnesene	SH	tr	tr	RI, MS
1509	1508	Germacrene A[f]	SH	/	/	RI, MS
1515	1513	γ-Cadinene	SH	tr	tr	RI, MS
1520	1522	δ-Cadinene	SH	tr	tr	RI, MS
1543	1544	α-Calacorene	SH	tr	/	RI, MS
1579	1574	Germacrene D-4-ol	SO	tr	/	RI, MS
1585	1582	Caryophyllene oxide	SO	2.5	2.7	RI, MS, Co-GC
1611	1608	Humulene epoxide II	SO	tr	tr	RI, MS
1640	1639	Caryophylla-4(12),8(13)-dien-5α-ol[f]	SO	tr	/	RI, MS
1646	1640	*epi*-α-Murrolol	SO	tr	/	RI, MS
1657	1652	α-Cadinol	SO	tr	tr	RI, MS
1736	1739	Oplopanone[f]	SO	tr	/	RI, MS
1840	1840	Hexahydrofarnesyl acetone	O	tr	tr	RI, MS
1960	1959	Hexadecanoic acid	FAD	tr	/	RI, MS, Co-GC
2300	2300	Tricosane[f]	FAD	tr	tr	RI, MS, Co-GC
2400	2400	Tetracosane[f]	FAD	tr	tr	RI, MS, Co-GC
2500	2500	Pentacosane	FAD	tr	tr	RI, MS, Co-GC
2700	2700	Heptacosane	FAD	tr	tr	RI, MS, Co-GC
2900	2900	Nonacosane	FAD	tr	tr	RI, MS, Co-GC
3000	3000	Triacontane	FAD	tr	tr	RI, MS, Co-GC
3100	3100	Hentriacontane[f]	FAD	tr	tr	RI, MS, Co-GC
3300	3300	Tritriacontane[f]	FAD	tr	tr	RI, MS, Co-GC
		Total		**98.1**	**97.9**	
		Total monoterpenes		85.9	84.2	
		Monoterpene hydrocarbons (MH)		0.6	0.3	
		Oxygenated monoterpenes (MO)		85.3	83.9	
		Total sesquiterpenes		10.8	12.7	

(*continued on next page*)

Table 1 (*continued*)

RI_{exp}[a]	RI_{lit}[b]	Compound	Class[c]	Percentage (%)[d]		Identification[e]
				MO-1	MO-2	
		Sesquiterpene hydrocarbons (SH)		8.3	10.0	
		Oxygenated sesquiterpenes (SO)		2.5	2.7	
		Fatty acid and fatty acid-related compounds (FAD)		1.4	1.0	
		Others (O)		tr	tr	

*Literature linear retention indices on an apolar BP-1 column.

[a] RI_{exp} – experimentally determined linear retention indices on a DB-5MS column; experimentally determined linear retention indices on an HP-Innowax FSC column are given in Table S1 in the Supplementary material.

[b] RI_{lit} – literature RI values; the list of references for literature RI values is given in Table S1 in the Supplementary material.

[c] For compound class abbreviations, see the last rows of this Table.

[d] Values are means of triplicate analyses; tr – trace amounts (< 0.05%); /– not detected; RI and MS data for the detected but unidentified constituents of the herein analyzed essential oils are given the Supplementary material.

[e] RI – retention indices matching with literature data, MS – mass spectra matching, Co-GC – co-injection with a pure reference compound.

[f] Compound reported here for the first time as a constituent of *M. officinalis* essential oil.

[g] *n*-Octane is a frequently used industrial solvent and since found in traces it could be an impurity. All batches of the essential oil from this producer contained octane.

standards, as well as those from Wiley7, NIST14, MassFinder 2.3, and a homemade MS library with the spectra corresponding to pure substances, and, wherever possible, by co-injection with an authentic sample (see Table 1, column Identification).

2.7. Evaluation of acute toxicity in Artemia salina

The method for the evaluation of acute toxicity to brine shrimps (*Artemia salina*) was previously described by Radulović et al. (2015a). Freshly hatched nauplii were transferred from the hatching beaker into Petri dishes containing the tested compounds dissolved in dimethyl sulfoxide (DMSO) and diluted with artificial seawater. Final concentrations of the tested samples were as follows: 0.125, 0.0625, 0.03125, 0.01563, 0.0078 and 0.0039 mg mL^{-1}, whereas the final concentration of DMSO was 0.05% (*v/v*). DMSO was inactive under the stated conditions as demonstrated by a negative control. Dead nauplii were counted after 24 h and LC_{50} values (concentration lethal to 50% of nauplii) were determined. Sodium dodecyl sulfate (SDS) was used as the positive control. All the tests were performed in triplicate and repeated twice.

2.8. Animal in vitro and in vivo studies

2.8.1. Animals and housing

Disease and pathogen-free female BALB/c mice (20–25 g) were obtained from the Vivarium of the Institute of Biomedical Research, Medical Faculty, Niš, Serbia. The animals were maintained under standard husbandry conditions with a temperature of 23 ± 2 °C, relative humidity 55 ± 10% and 12/12 h light/dark cycle. All animals were fed with standard (commercial) laboratory food pellets and water was provided *ad libitum*. Animals were allowed to acclimatize to the laboratory environment for 7 days before initiating the experiments. The experiments were performed at the Institute of Biomedical Research, Medical Faculty, Niš, Serbia, and were in accordance with the declaration of Helsinki and European Community guidelines for the ethical handling of laboratory animals (EU Directive of 2010; 2010/63/EU), and were performed after the experimental protocols were approved by the animal ethics committee of the Republic of Serbia (decision No: 323-07-06862/2016-05/19).

2.8.2. Primary mouse cell culture isolation and treatment

The isolation of thioglycolate-elicited macrophages (Mø) and spleen lymphocytes (splenocytes; SPCs) was performed following previously described protocols (Radulović et al., 2014, 2016). After cell harvesting, their density was adjusted to 2.5×10^6 cell mL^{-1} of RPMI medium, the viability was confirmed using Trypan blue staining (> 95% of viable cells) and the cells were seeded into 96-well plates (100 μL/well). The test substances (*M. officinalis* essential oil, citronellal, and a mixture of citrals) were initially dissolved in DMSO and further diluted with RPMI medium (less than 0.5% (*v/v*) of DMSO per well) to obtain the final concentrations. Further incubation of cells with *M. officinalis* essential oil (100–0.01 μg mL^{-1})/citronellal (10^{-4} – 10^{-8} M)/the mixture of citrals (10^{-4} – 10^{-8} M)/dexamethasone (10^{-4} M; Dex)/RPMI medium was performed at 37 °C for 24 h under the atmosphere of 95% air and 5% CO_2 (*v/v*). All experiments were done in quadruplicate and repeated three times.

2.8.3. Viability assay and cell appearance

After the incubation time elapsed fresh RPMI medium and 10 μL of MTT solution were added to all wells and the plates were incubated for additional 4 h. Formed dark blue crystals were dissolved using acidic isopropanol (0.04 M HCl in isopropanol) and a few minutes after the dissolution, the absorbance was measured at 550 nm (Radulović et al., 2016) using an automated microplate reader (Multiscan Ascent, Labsystems, Helsinki, Finland). The obtained results, % of viability relative to the RMPI-cultured cells, are presented as the mean ± standard deviation (SD). Cell appearance after the incubation period was assessed using a light microscope Zeiss observer Z1 (Carl Zeiss, Göttingen, Germany), at magnification 400x. The number, shape, morphological characteristics, presence of apoptotic cells/bodies in the cell cultures was determined/evaluated.

2.8.4. Evaluation of in vivo acute toxicity

2.8.4.1. Essential-oil application and median lethal dose (LD_{50}) calculation. Mice, divided into groups of 5 animals, were orally (*p.o.*) treated with the essential oil of *M. officinalis*, dissolved in olive oil, in increasing doses from 500 to 3000 mg kg^{-1}. After the application, the animals were monitored continuously during the first 2 h, and occasionally within the next 4 and 24 h (Radulović et al., 2013b). Before the animals were sacrificed, blood was taken from the retro-orbital plexus and used for the serum biochemical analysis. In some cases, instantly after animal death, necropsy was performed (during the first 4 h of the observation period), and organs (liver, kidneys, stomach, and duodenum) were removed, while for the remaining, surviving animals, after blood collection and sacrifice, organ removal was performed. The median lethal dose (LD_{50}) calculation was done using the Probit analysis (Radulović et al., 2013b).

2.8.4.2. Measurement of serum biochemical parameters. After the blood was withdrawn, it was allowed to clot at room temperature and the

serum was separated after centrifugation at 3000 rpm for 10 min. Serum levels of biochemical parameters reflecting liver (aspartate transaminase (AST), alanine transaminase (ALT), γ-glutamyl transferase (γ-GT), alkaline phosphatase (ALP), and albumin (ALB)) and kidney (creatinine (CRE) and urea) function, and glucose were evaluated using an Olympus AU680® Chemistry-Immuno Analyzer (Olympus America Inc., USA). According to the criteria of the World Health Organization Adverse Reaction Terminology, the likelihood of drug-induced, in our case essential oil-induced, adverse hepatic event in mice (Lenaerts et al., 2005) was estimated based on ALT levels. Grades of hepatotoxicity were defined as follows: grade I with serum levels of ALT from 51 to 125 IU L^{-1} (or 1.25–2.5 times normal values), grade II with serum levels of ALT from 126 to 250 IU L^{-1} (or 2.6–5.0 times normal values), grade III with serum levels of ALT from 251 to 500 IU L^{-1} (or 5.1–10.0 times normal values) and grade IV with serum levels of ALT > 500 IU L^{-1} (or > 10.0 times normal values).

2.8.4.3. Histopathological and immunohistochemical analysis. The harvested liver, kidney, stomach, and duodenum tissue specimens were washed in isotonic phosphate buffer saline (PBS) and fixed in 10% paraformaldehyde (in 0.1 mol L^{-1} phosphate buffer saline), dehydrated with solutions of ascending ethanol concentration (50–100%, *v/v*), and embedded in paraffin. Tissue samples were cut into 4–5 μm thick sections (HistoRange microtome; model: LKB 2218, LKB-Produkter AB, Bromma, Sweden) and stained standardly with hematoxylin and eosin (H&E). Special histochemical staining of liver and kidney tissues included the periodic acid-Schiff (PAS) staining, while the gastric and duodenal tissue samples were stained by following the alcian blue-periodic acid-Schiff (AB-PAS) protocol. For the immunohistochemical staining, a primary polyclonal 4-hydroxynonenal antibody (4-HNE, 1:200 dilution, Abcam) was used. The standard procedure of antigen retrieval (citrate buffer) and endogenous peroxidase blockage (using 3% hydrogen peroxide) was performed prior to an overnight incubation with the primary antibody in a moist chamber. The visualization was effectuated using diaminobenzidine and counterstained with Mayer's hematoxylin.

Stained tissue sections were further examined under an Olympus BH2 light microscope (Olympus America Inc., USA) by two independent researchers (I.I. and V.P.) unaware of the nature of the treatment in order to determine the extent of tissue damage following the application of the essential oil. The liver and kidney morphological changes, performed on H&E stained tissue, were graded as 0 (no change), 1 (slight/mild changes; < 30%), 2 (moderate; 30–50%) and 3 (severe; > 50%). Determination of glycogen amount present in the liver tissue was performed on PAS-stained liver tissue sections, while the presence of tubular casts, was additionally examined on PAS-stained kidney sections. The existence of gastric and/or duodenal lesions was scored as previously described (Radulović et al., 2013c) and the changes in the amounts of neutral/acidic glycoproteins in these parts of the gastrointestinal system was scored on AB-PAS stained tissue sections (0 (no change), 1 (slight/mild changes; < 30%), 2 (moderate; 30–50%) and 3 (severe; > 50%)). Immunohistochemical positivity was analyzed on stained tissues and the presence of dark/brown coloration within the cells was scored as 0 (no immuno-positivity present), 1 (slight/mild immuno-positivity; < 30%), 2 (moderate immuno-positivity; 30–50%) and 3 (high immuno-positivity; > 50%).

2.8.4.4. Tissue biochemical parameters determination

2.8.4.4.1. Malondialdehyde determination. The determination of the extent of tissue lipid-peroxidation was based on the amount of the formed malondialdehyde (MDA) estimated by a spectrophotometric method (monitored wave length 532 nm), using the thiobarbituric acid reaction (Buege and Aust, 1978). The amount of tissue MDA was expressed as nmol mg^{-1} of tissue proteins.

2.8.4.4.2. Catalase activity determination. Tissue catalase (CAT) activity was determined using hydrogen peroxide (H_2O_2) as the substrate, whereafter the incubation period, the reaction was stopped by the addition of the chromogen ammonium molybdate (Goth, 1991). The absorbance was measured at 405 nm and the results were expressed as IU mg^{-1} of proteins.

2.8.4.4.3. Myeloperoxidase activity determination. Myeloperoxidase (MPO) activity was determined in tissue homogenates using *o*-phenylenediamine activated with H_2O_2 as described previously (Radulović et al., 2014). Shortly, after the incubation, the reaction was stopped with an H_2SO_4 solution and optical densities (OD) were determined at 540 nm using the mentioned microplate reader. The results are expressed as OD mg^{-1} of proteins.

2.8.4.4.4. Reduced glutathione concentration determination. Tissue reduced glutathione (GSH) was estimated using a standard method previously described by Ellman (1959). After mixing the tissue homogenate with 5% (*w/w*) trichloroacetic acid, the mixture was centrifuged and the clear supernatant was further used. The supernatant and DTNB reagent [5,5-dithiobis(2-nitrobenzoic acid)] were incubated for 30 s and the absorbance of the reaction was measured at 412 nm. The amount of GSH was determined based on the standard curve and expressed as μmol of GSH g^{-1} of tissue.

2.8.4.4.5. Tissue NO_2^- concentration determination. The concentration of nitrites present in the tissue homogenates was measured using the Griess reagent (Radulović et al., 2015b). The mixture consisting of tissue homogenate and Griess reagent was incubated at room temperature for 10 min and the absorbance was measured at 540 nm using the microplate reader. The total nitrite concentrations were calculated using a standard curve of sodium nitrite.

2.9. Statistical analysis

The results were expressed as the mean ± SD and for each of the evaluated biochemical parameters, the confidence interval (C.I.) of 95% was calculated. Statistically significant differences between the treatments in *in vitro* assays were determined by One-Way Analysis of Variance (ANOVA) followed by Tukey's post-hoc test for multiple comparisons (GraphPad Prism version 5.03, San Diego, CA, USA). Probability values ($p \leq 0.05$) were considered to be statistically significant.

3. Results and discussion

3.1. Chemical composition of *M. officinalis* essential oil

Detailed GC-MS and GC-FID analyses of *Melissa officinalis* essential-oil samples, isolated from the aerial parts (sample **MO-1**) and a commercial one (sample **MO-2**), Table 1, permitted the identification of, in total, 133 essential-oil constituents that represented 97.9–98.1% of the total detected GC-peak areas. Fig. 1 shows a typical total ion chromatogram (TIC) of *M. officinalis* essential-oil sample (**MO-2**). Terpenoids comprised 93.6 and 94.8% of **MO-1** and **MO-2**, respectively, with oxygenated monoterpenes as the most abundant compound class (82.1–82.8%). The oils were mainly comprised of acyclic monoterpenoids with citronellal (21.2–21.8%), neral (17.8–18.4%), and geranial (22.9–23.5%) as the major constituents. Interestingly, monoterpene hydrocarbons contributed less than 1% of the essential-oil samples (0.3–0.6%). The remaining part of the oil samples was comprised of sesquiterpenoids, fatty acid-related and carotenoid-derived compounds 10.8–12.7%, 1.0–1.4%, and 2.0–2.9%, respectively. There were, in general, only small quantitative differences observed between **MO-1** and **MO-2** samples. Variations of the percentage content were in the range 0–1.3%, e.g., the content of citronellal, neral, and geranial, the main essential oil constituents, varied within ≈3% from one essential-oil sample to the other (Table 1).

Although 26 compounds are reported here for the first time as constituents of *M. officinalis* essential oil, the chemical composition was

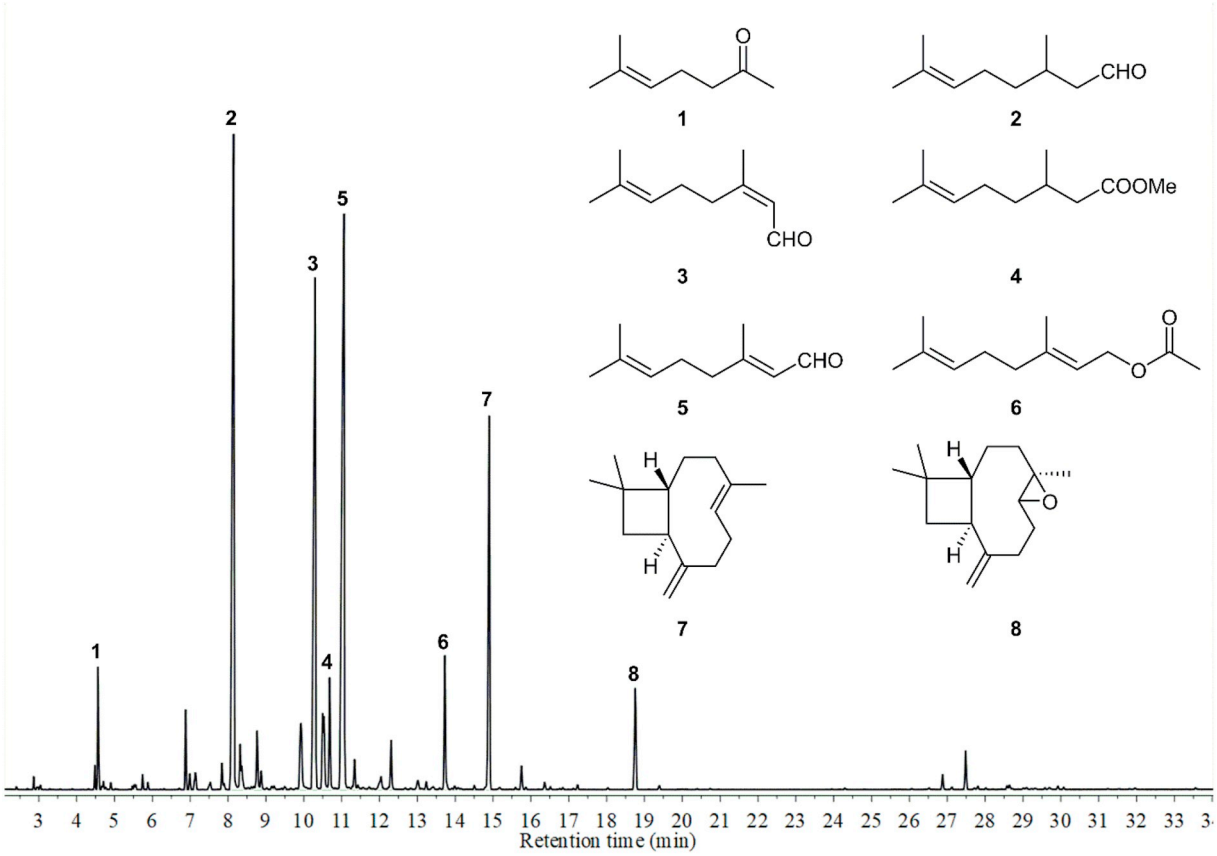

Fig. 1. Typical TIC (Total Ion Current) chromatogram of *M. officinalis* essential oil (sample **MO-2**). **1**, 6-Methyl-5-hepten-2-one; **2**, citronellal; **3**, neral; **4**, methyl citronellate; **5**, geranial; **6**, geranyl acetate; **7**, (*E*)-caryophyllene; **8**, caryophyllene oxide.

more or less qualitatively comparable, at least with respect to the major constituents, to previous reports on *M. officinalis* essential oil with citronellal and both stereoisomers of citral (geranial and neral) as the main oil constituents (Nurzyńska-Wierdak et al., 2014; Sharopov et al., 2013; Verma et al., 2015). The composition of *M. officinalis* essential oil is known to depend on the exact taxonomical origin of the plant material, more specifically on the subspecies in question. The essential oil of the typical subspecies, *M. officinalis* ssp. *officinalis* is characterized by significant amounts of citrals and/or citronellal, whereas *M. officinalis* ssp. *altissima* contains only minor amounts of these compounds. The *altissima* subspecies essential oil is rich in terpene hydrocarbons, more precisely, the sesquiterpenes β-caryophyllene and germacrene D, and the monoterpenes sabinene and β-pinene (Chizzolla et al., 2018). Occasionally, higher relative amounts of caryophyllene oxide were detected (Basta et al., 2005). Our samples clearly belong to the typical subspecies essential oils, renown and used widely. Such phytochemical variation between subspecies is expected to have an important influence on various medicinal/pharmaceutical traits of the plant material and the absence of monoterpene aldehydes (geranial, neral, and citronellal) with proven biological/pharmacological properties (Shakeri et al., 2016; Ulbricht et al., 2005) would be most detrimental.

The main detected essential-oil constituents (citronellal, neral, and geranial) were quantified (mg per g of the essential-oil sample) by constructing a calibration curve. The calibration curves of areas under the GC-FID peaks plotted against the concentration had excellent correlation coefficients, higher than 0.9998. These analyses revealed that 1.0000 g of *M. officinalis* essential-oil samples **MO-1** and **MO-2** contain 155 and 159 mg of citronellal and 425 and 427 mg of a mixture of (*Z*) and (*E*)-citral, respectively. Since the commercial sample (**MO-2**) corresponded well to the one isolated by us from the at hand plant material (**MO-1**), we opted to use only the commercial sample in further toxicity testing since a much larger quantity of **MO-2** was available to us.

3.2. *In vitro* toxicity

3.2.1. *Artemia salina* toxicity

Initially, the *in vitro* toxic potential of *M. officinalis* essential oil (**MO-1**), citronellal and the mixture of geranial and neral (citrals) was investigated using the brine shrimp lethality assay. This assay is suitable for a preliminary detection of toxic compounds towards eukaryotic cells (Radulović et al., 2017). The calculated LC_{50} values after a 24 h treatment, for the corresponding essential oil and the monoterpene aldehydes, were: 38.6, 28.3, and 16.8 mg L^{-1}, for *M. officinalis* essential oil, citronellal, and citral, respectively. Essential oils and their constituents are known to be both highly toxic (LD_{50} around 20 μg mL^{-1}) or practically non-toxic, while the toxicity of essential oils is, logically, highly dependent on its composition (Radulović et al., 2013b, 2015a, 2017). Both citronellal and citrals were more toxic for *A. salina* than the same mass of the essential oil containing them. Assuming additivity of the toxicities of the constituents, a mixture of the monoterpene aldehydes and other supposedly non-toxic constituents present in the essential oil tested would have a LD_{50} *ca.* 34 mg L^{-1}. It appears that the overall noted toxicity is close to this value but that also other factors, antagonistic interactions between oil constituents, might be responsible for the net result. Previously, *Cymbopogon nardus* essential oil, which shares the same main constituents with *M. officinalis* oil, was shown to possess a relatively low LD_{50} value (12.4 μg mL^{-1}) in the brine shrimp lethality assay. It is some three times more toxic than the *M. officinalis* essential oil obtained in our study, and although this seems reasonable since the mentioned *C. nardus* essential oil possesses two times more citronellal than the here-tested essential oil (Olivero-Verbel et al., 2010), this is not enough to explain such a low LD_{50} value, meaning that other

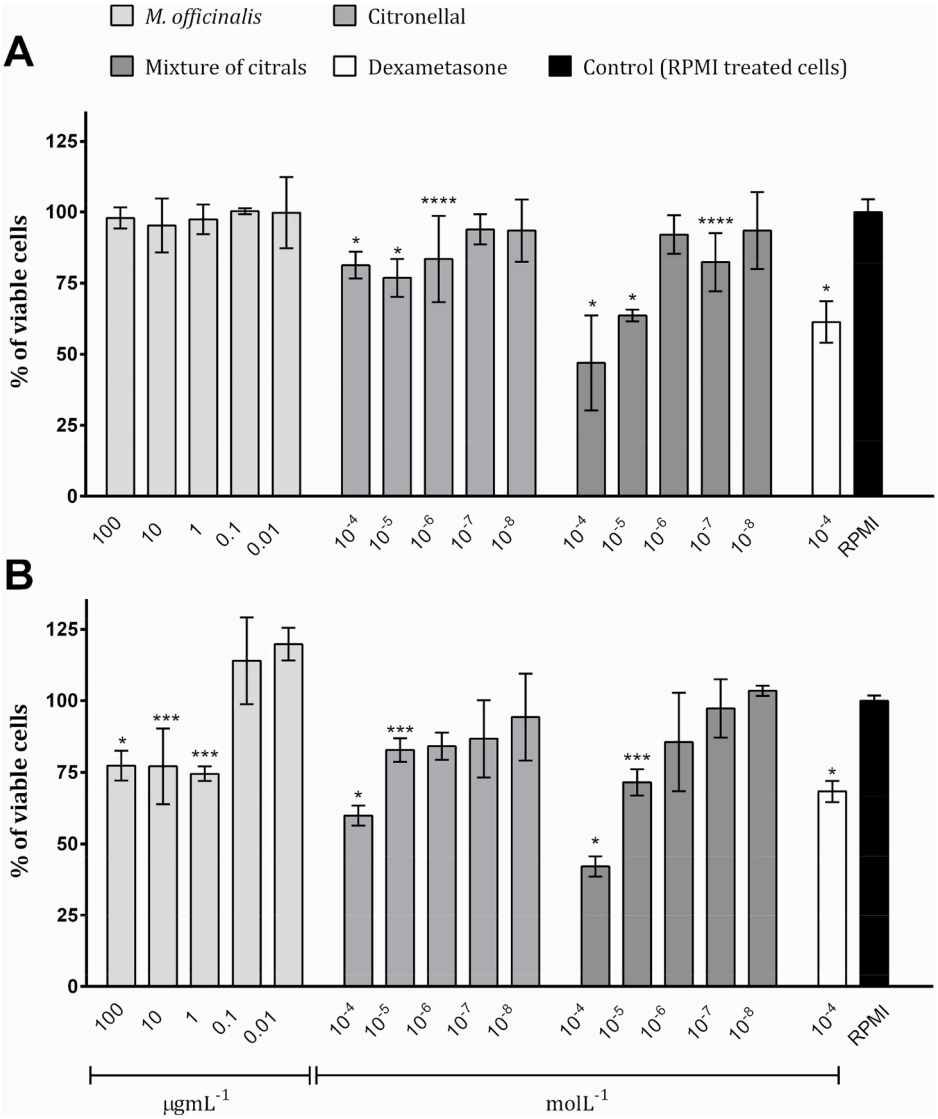

Fig. 2. Effect of *Melissa officinalis* essential oil, citronellal, a mixture of citrals, and dexamethasone on macrophage (A) and SPC (B) viability, compared to the survival of cells in RPMI-medium, estimated by the MTT assay. Data are presented as mean ± SD; the statistical significance was calculated by One-Way ANOVA followed by Tukey's post hoc test. *$p < 0.0001$; ***$p < 0.01$; ****$p < 0.05$ vs. RPMI-treated cells.

constituents must contribute to the observed toxicity.

3.2.2. Macrophage and splenocyte viability and morphology under the influence of different treatments with M. officinalis oil, and its constituents

The essential oil of *M. officinalis* was assessed for its effect on the viability of isolated BALB/c mice peritoneal macrophages (Mø), and splenocytes (SPC) by an MTT test. Higher tested concentrations of *M. officinalis* essential oil caused a statistically significant reduction in splenocyte viability compared to the RPMI-treated cells (Fig. 2). On the other hand, the essential oil tested in the same concentration range did not affect macrophage viability (Fig. 2). Both citronellal and the mixture of citrals produced a statistically significant decrease in the amount of reduced MTT present in both macrophage and splenocyte cultures (Fig. 2). Similar percentage of cell viability reduction was seen in the treatment with the positive control, dexamethasone (Dex, Fig. 2).

There are no previous studies on the effect of *M. officinalis* essential oil on cell viability. Since essential-oil constituents can be found in different solvent extracts, we can, not completely appropriately, only discuss our results in the light of the results reported for these extracts. Previous studies showed that different extracts of *M. officinalis* possess a certain degree of cytotoxicity at usually higher tested concentrations (Abudayyak et al., 2015; Bayat et al., 2012; Hassanzadeh et al., 2011). Namely, in concentration higher than 0.1 mg mL^{-1} a *M. officinalis* extract was proven to decrease cell metabolism and increase LDH release in primary BALB/c mice neuronal cultures (Bayat et al., 2012). A water extract, tested at concentrations higher than 0.1 mg mL^{-1}, was found to decrease Wistar rat-isolated hippocampal neuron viability (Hassanzadeh et al., 2011). Chloroform and methanol extracts of *M. officinalis* exhibited, at relatively high concentrations (several mg mL^{-1}) both cytotoxicity and genotoxic properties towards rat kidney cells and *Salmonella typhimurium*, respectively (Abudayyak et al., 2015). The results of our study are generally in agreement with such previous findings, as only high concentrations cause significant effects and only decrease selected cell (SPCs) viability (Fig. 2B).

Under the experimental conditions of our study, cultures of untreated Mø showed characteristic cell morphology with predominantly round and occasional spindle-shaped cells (Fig. 3A). *Melissa officinalis* essential-oil treatment did not produce any changes in the number, volume of Mø or their appearance (generally seen as the round form). When citronellal or the mixture of citrals was applied, concentration-depended changes in Mø number and morphology were found. A significant portion of Mø appeared dead (detached cells) when the highest

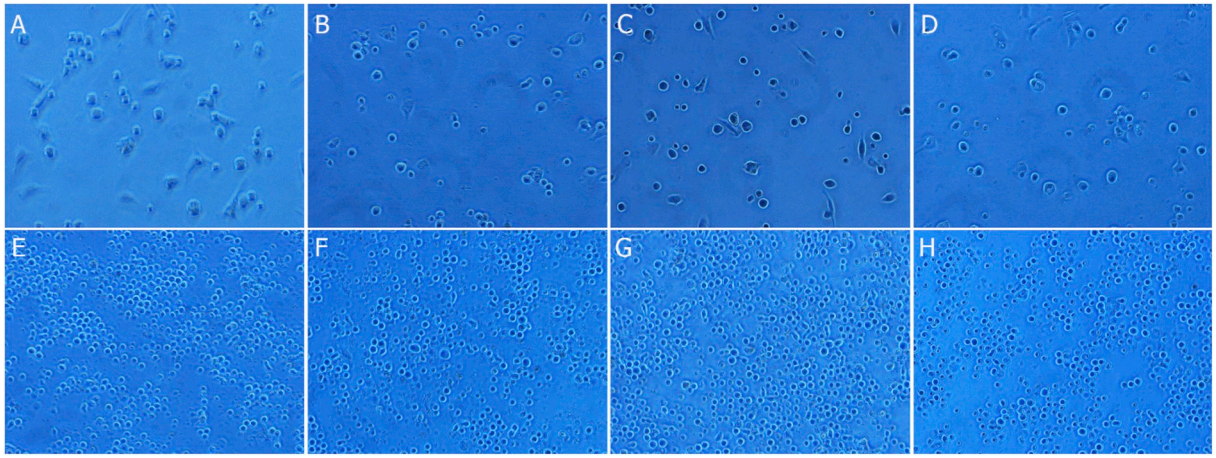

Fig. 3. Changes in macrophage (A-D; x400) and SPCs (E-H; x400) appearance under the influence of *Melissa officinalis* essential oil, citronellal, a mixture of citrals and dexamethasone. Normal, predominantly round, macrophage appearance (A), while under the influence of different treatment numerous detached (B) and apoptotic (C) macrophages with the reduction in their number (D) could be seen. Mostly large and occasional small round SPCs (E) in control treated cells were found, under the influence of different treatment several degrees of dead (F, G) and/or apoptotic (H) SPCs could be seen, with ones having their morphology/size altered as well (F–H).

concentration of citronellal/the mixture of citrals was added to the RPMI medium, while lower concentrations caused cell clumping and the reduction of their volume (Fig. 3B and C). In the cases where Dex was applied, Mø displayed reduced volume and membrane blebbing, and evident reduction in cell number (Fig. 3D). Spleen cell cultures treated with RPMI medium showed distinctive features of lymphocytes present in the spleen, mostly round cells different in size (small and large lymphocytes, Fig. 3E). Each of the treatments (essential oil/citronellal/mixture of citrals/Dex) led to a different extent of decrease in the number of and alteration in SPCs morphology (Fig. 3F–H). In these SPC cultures, cells with both reduced and increased (swollen) volume, clumped cells and those in apoptosis could be seen (Fig. 3F–H).

3.3. In vivo animal toxicity

3.3.1. Gross behavior changes

After the oral administration of *M. officinalis* essential oil to BALB/c mice, in a dose range from 0.5 to 3 g kg^{-1}, the first mortality was noticed around 1 h after the application of 1.5 g kg^{-1} dose. The calculated *p.o.* LD_{50} value for the essential oil, using Probit analysis, was 2.57 g kg^{-1}. Compared to other essential oils, it could be classified as moderately toxic (Radulović et al., 2012). Previous evaluation of *M. officinalis* essential oil toxicity in mice, in an acute model, suggested that its LD_{50} value lays above 2 g kg^{-1} and that there were no significant changes in animal behavior, general appearance or any signs of toxicity after a 2 g kg^{-1} application (Bounihi et al., 2014). In a subacute toxicity model in rats, 100 and 200 mg kg^{-1} of *M. officinalis* essential oil application produced only a mild kidney damage, observed both through an increase in blood urea levels and microscopic tissue damage in the form of glomerular ischemic lesions and minimal focal tubular necrosis (Bounihi et al., 2014). The determined oral rat LD_{50} value for *Cymbopogon citratus* essential oil, whose composition is similar to the one of *M. officinalis* oil (however, without citronellal), was shown to be 3250 mg kg^{-1} of body weight, where no behavior abnormalities were observed when doses below 2 g kg^{-1} were applied (Fandohan et al., 2008).

Lower applied doses (up to 1.5 g kg^{-1}) of the oil decreased animal movement, produced abdominal writhings, tumbling, atony, spastic movements and in some cases muscle rigidity. With the increase of oil doses the symptoms of intoxication were more pronounced, developed faster and additional ones arose: tremor, loss of balance (without loss of righting reflex), the complete absence of movement, hyperventilation, and spontaneous vocalization. Interestingly, these results are not in accordance with the previous publication, where no behavior alterations, except for a slight reduction in the locomotor activity, were found following the essential-oil application in a dose of 2 g kg^{-1} (Bounihi et al., 2014). Although CNS is protected by the blood-brain barrier, essentially this barrier consists of tight junctions that exist between endothelial cells (McQueen, 2010), the lipophilicity of essential oil constituents enables them to pass this barrier via the cell membrane. Thus, one could expect the changes in symptom intensity to accompany the change in the dose of essential oil.

The effect of significantly lower doses of *M. officinalis* extracts on CNS functioning has been investigated and these were revealed to possess a dose-dependent sedative, sleep-inducing and pentobarbital-potentiating effects. Interestingly, in the same study, the effects of the

Table 2
Effects of high doses (1–3 g kg^{-1}) of *M. officinalis* essential oil on female BALB/c serum biochemical parameters.

Dose (g kg^{-1}) Biochemical parameter	ALT (U L^{-1})	AST (U L^{-1})	ALP (U L^{-1})	γ-GT (U L^{-1})	ALB (g L^{-1})	Urea (mmol L^{-1})	CRE (μmol L^{-1})	Glucose (mmol L^{-1})
1	32.0 ± 5.6	145.5 ± 13.4	81 ± 11	3 ± 0.1	15.2 ± 0.2	6.3 ± 0.4	10.5 ± 0.7	7.2 ± 0.1
1.25	155 ± 125	301 ± 192	91.5 ± 33.8	4 ± 0.3	14.8 ± 1.6	11.9 ± 8.5	20.5 ± 7.9	5.5 ± 1.3
1.5	89.0 ± 49.8	207.1 ± 80.8	88.1 ± 26.2	3.7 ± 0.7	15.2 ± 1.3	9.6 ± 4.6	17.0 ± 1.4	6.4 ± 0.9
2	41.0 ± 5.6	134.5 ± 11.2	68.3 ± 2.7	4.5 ± 0.7	14.0 ± 0.3	8.3 ± 4.1	15 ± 1.6	4.3 ± 0.6
3	77.5 ± 23.5	165.5 ± 19.1	119.5 ± 4.2	3.5 ± 0.7	14.9 ± 0.4	15.6 ± 3.2	24.5 ± 8.6	5.2 ± 0.8
Vehicle (10 mL kg^{-1})	35.3 ± 6.2	130 ± 16.1	78.7 ± 6.7	2.7 ± 0.8	16.3 ± 1.2	7.2 ± 0.7	3.1 ± 2.6	5.9 ± 0.7
C.I. 95%	31.1–39.6	118.8–141.2	73.1–84.3	2.1–3.2	15.4–17.1	6.7–7.6	1.3–4.9	5.4–6.4

Data are given as mean values ± SD.

Table 3
The degree of histopathological changes of mice livers, kidneys, stomachs and duodenums after exposure to different doses of *M. officinalis* essential oils.

Histopathological finding[a]		Dose (g/kg)					
		0	1	1.25	1.5	2	3
Liver	Cytoplasmic micro vacuolization	0.5	1.5	1.3	1.75	1.5	1.5
	Parenchymatous degeneration	0.0	1.0	1.25	1.5	1.5	1.75
	Vascular congestion	0.0	1.7	1.0	1.25	2.25	2.0
	Sinus spaces narrowing	0.0	0.7	1.0	1.0	1.0	0.7
	Activated Kupffer cells	1.0	2.0	2.0	2.5	2.0	1.0
	Eosinophilic infiltration	0.0	1.5	0.6	2.0	1.5	1.5
	Hypereosinophilic areas	0.0	1.5	1.0	1.25	1.25	2.25
	Karyopyknosis	0.0	0.5	1.0	0.75	0.75	1.75
	Changes in glycogen content	0.0	1.0	1.0	1.2	0.75	1.0
	4-HNE-positivity	0.2	0.2	0.5	0.75	1.5	2.0
Total score		*1.7*	*11.6*	*10.7*	*14.0*	*14.0*	*15.4*
Kidney	Glomerular hypertrophy	0.0	1.8	1.4	2.25	1.7	2
	Glomerular cellularity	0.0	0.5	0.0	0.0	0.0	0.0
	Peritubular infiltration	0.0	0.8	1.1	1.5	2.0	2.0
	Perivascular infiltration	0.0	1.0	0.6	0.0	0.0	0.5
	Protein cast	0.0	1.0	2.3	2.0	2.0	2.0
	Cloudy swelling	0.25	1.0	1.6	2.0	2.25	2.25
	Tubule cell vacuolization	0.0	0.25	0.25	0.5	0.75	0.5
	Hemorrhage	0.0	1.0	0.0	0.0	2.0	0.0
	PAS-positive cast	0.0	1.0	1.1	1.5	2.0	2.25
	4-HNE-positivity	0.0	0.0	0.75	0.5	1.0	0.75
Total score		*0.25*	*8.35*	*9.1*	*10.2*	*13.7*	*12.3*
Stomach	Single spotted erosions	0.0	0.0	0.0	0.0	0.0	0.0
	Glandular cell vacuolization	0.0	0.0	0.5	0.25	0.2	0.25
	Inflammatory cells infiltration	0.0	0.25	0.0	0.5	1.25	1.5
	Capillary vasodilatation	0.0	0.0	0.0	0.0	0.5	0.75
	PAS-positive mucus	0.0	0.0	0.5	1.0	1.5	1.25
	AB-positive mucus	0.0	0.0	0.0	0.7	0.7	1.0
	4-HNE-positivity	0.0	0.0	0.2	0.5	1.5	2.0
Total score		*0.0*	*0.25*	*1.2*	*2.9*	*5.6*	*6.8*
Duodenum	Inflammatory cells infiltration	0.5	0.75	1.0	0.7	0.5	0.75
	Capillary vasodilatation	0.0	0.5	0.75	0.5	0.75	1.0
	Interstitial edema	0.0	0.5	0.5	0.5	0.5	0.75
	Villi necrosis	0.0	0.2	1.0	0.75	1.5	1.5
	AB-positive mucus	0.0	0.5	0.5	2.0	1.5	1.5
	4-HNE-positivity	0.0	0.25	0.5	0.5	1.0	1.5
Total score		*0.5*	*2.7*	*4.2*	*4.9*	*5.8*	*7.0*

[a] Values of the histopathological score are given as the mean of n = 4–5.

essential oil, applied intraperitoneally, on CNS were not proven (Ulbricht et al., 2005). On the other hand, the oral application of *M. officinalis* essential oil produced sedative and narcotic effects, in mice, at doses of 3.16 mg kg^{-1} and higher (ESCOP, 2003). This implies that the essential-oil constituents might undergo a chemical transformation in the gastrointestinal system into CNS affecting substances that do not take place when the essential oil is applied intraperitoneally. Previous reports on the intraperitoneal toxicity of citronellal, one of the major oil constituents, in male/female NMRI mice showed that the LD_{50} is somewhere between 200 and 700 mg kg^{-1} (ECHA). Gross pathological analysis revealed no intra-abdominal precipitations or adhesions; however, no further findings (i.e. microscopic evaluation of organ changes) were reported. Signs of intoxication, similar to those found after the application of higher essential oil doses, included: apathy, abnormal body position, tumbling, atony, spastic movements, tonic/clonic convulsions, paresis and poor general condition (ECHA). Additionally, the mixture of geranial and neral (citral) is known to dose-dependently inhibit retinoic acid synthesis, affecting fetal development (Tisserand and Young, 2014).

3.3.2. Serum biochemical parameters

The high doses of the essential oil caused a marked increase, above the upper confidence interval (C.I.) values for healthy untreated mice, in serum biochemical parameters reflecting liver and kidney function (Table 2). Almost all applied doses produced a certain degree of tissue damage that is seen in the serum biochemical parameters levels. Additionally, a mild impact on serum glucose levels was observed, where only the dose of 1 g kg^{-1} of essential oil slightly increased glucose levels (Table 2). This finding seems opposite to the data from a previous publication which showed that *M. officinalis* essential oil reduces blood-glucose levels, possibly by increasing insulin levels (Chung et al., 2010). However, in the work of Chung et al. (2010), the essential oil was applied to mice suffering from diabetes type 2, on more than one occasion, thus the discrepancy in effect on glucose levels might not be unexpected.

Liver function, estimated via the serum levels of liver transaminases, was significantly impaired with the increase in the amount of *M. officinalis* essential oil applied. Destruction of hepatocytes can be directly linked to the concentrations of ALT, leaked from damaged cells, in the serum (Lin and Wang, 1986). By looking at ALT levels, one can say that the liver well tolerated high doses of the essential oil, with an

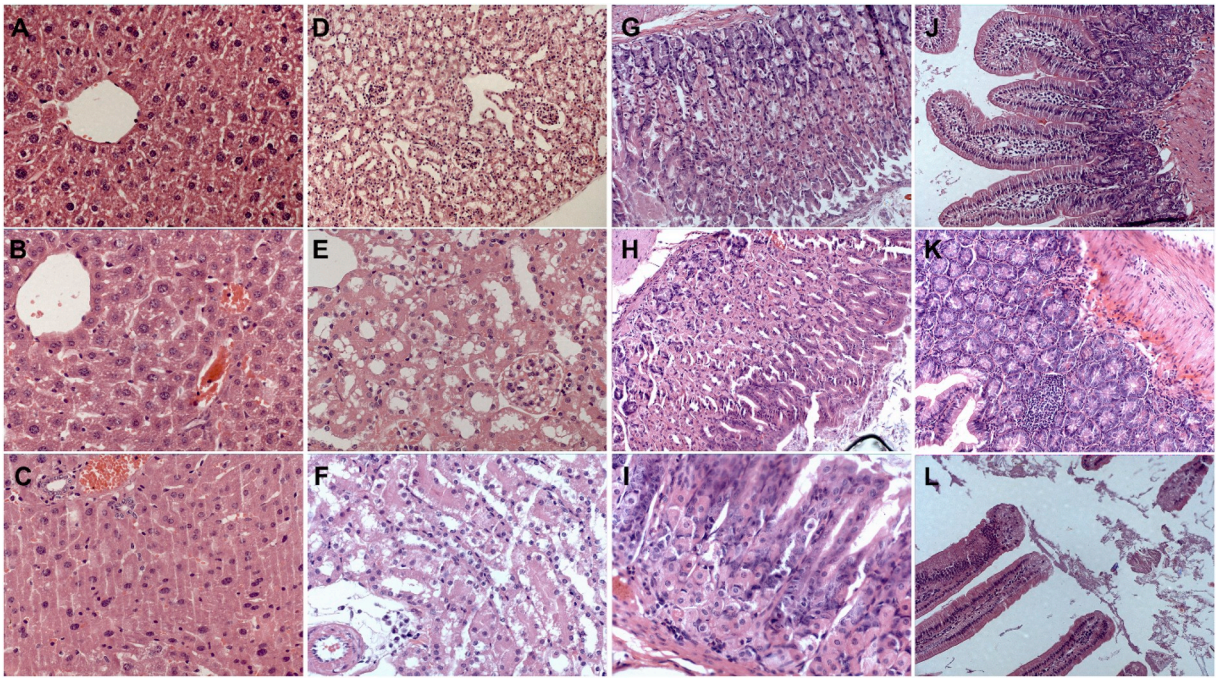

Fig. 4. Changes in liver (A–C), kidney (D–F), stomach (G–I) and duodenum (J–L) microscopic appearance after *Melissa officinalis* essential oil application. Normal liver lobular architecture, with well-defined cellular structures (A; x400); Zonal distribution of hepatocyte changes (parenchymatous degeneration) and stasis (B; x400), with hepatocytes having hypereosinophilic cytoplasm (C; x400), was seen in the liver of animals treated with essential oil. Kidney structures from untreated animals showed normal morphology with well-defined tubules and glomeruli (D; x400); In the renal cortex of mice exposed to increasing doses of essential oil glomerular hypertrophy, tubular cell vacuolization and degeneration (E; x400) with areas of proximal/distal tubular edema (F; x400) could be seen. Preserved glandular architecture, free from any pathological changes could be seen in a control group of animals (G; x200), while in those treated with increasing doses of essential oil inflammatory cells (H; x200) and capillary dilation and edema (I; x400) could be seen occasionally. Duodenal mucosa with normal long, finger-like vill in the control group of animals (J; x200); In animals treated with different doses of essential oil the dose-dependent changes included inflammatory cell infiltrate (K; x200) and villi tip necrosis (L; x200).

occasional extreme single value of ALT within the animal group. According to the WHO criteria for hepatotoxicity estimation, the serum ALT levels were found to be first grade (mostly ≈ 2-fold increase) for a single mouse within the groups for all doses, and for only one animal that received 1.25 g kg^{-1} the increase was found to be grade II. Additionally, the liver synthetic function, which is connected to ALB levels (Thapa and Walia, 2007) was not affected by the application of the essential oil (Table 2). Similarly, only the highest tested dose of the essential oil caused a significant increase in ALP. However, it was previously found that liver cytochrome P-450 enzymes 2B1 and 2B6, both rat and human forms, were inhibited by citral in concentrations around 2 μM (Tisserand and Young, 2014). These two isoforms are essential for cytostatics (cyclophosphamide), opioids (methadone), anticonvulsants (valproate), antidepressants (bupropion) and anesthetics (ketamine) metabolism, thus the application of *M. officinalis* essential oil containing larger amounts of citrals could significantly influence drug metabolism (Tisserand and Young, 2014).

Increased AST serum levels could be linked to liver and/or muscle tissue damage (Weibrecht et al., 2010). The increase in serum AST levels of mice treated with high doses of *M. officinalis* essential oil was evident (Table 2), indicating possible toxic liver damage. However, since the levels of ALT, a more sensitive marker of liver damage, are not exceeding 200 U L^{-1} (Johnston, 1999), one cannot claim that liver is the main target tissue for *M. officinalis* essential-oil toxicity. Also, since the abovementioned signs of intoxication included muscle rigidity and spastic movements, with some additional muscle-related symptoms, a certain mild degree of rhabdomyolysis that contributes to the serum AST levels (Keltz et al., 2013) could be expected.

The applied essential oil in doses higher than 1.25 g kg^{-1} increased serum levels of γ-GT above the upper C.I. value (Table 2). The increase in serum levels of this membrane-bound enzyme, mainly localized in the liver and kidneys, represents a potential marker of oxidative tissue damage that is known to occur after an application of alcohol or heavy metals (Lee et al., 2004). Thus, one may speculate that the essential oil cased a certain degree of liver/kidney oxidative damage. The enzyme's main function is to metabolize extracellular GSH providing free amino acids for GSH intracellular synthesis, thus its expression and tissue activity is closely related to GSH content (Lee et al., 2004).

Acute kidney injury can be estimated based on the elevation in urea and CRE serum levels. These two parameters were increased by all applied doses of the essential oil (Table 2), suggesting kidney damage. The levels of CRE are known to be more specific in the early phase of kidney damage, while urea concentrations start to increase after significant renal parenchymal damage and it does not significantly increase until glomerular filtration rate is diminished by 50% (Ahmed et al., 2015). In the mentioned previous sub-acute toxicity study, 3 months after a daily injection of *M. officinalis* essential oil (100 and 200 mg kg^{-1}) to rats, changes in urea levels were detected (Bounihi et al., 2014). However, the increase in CRE levels was much higher compared to urea. These results contribute to the hypothesis of a potential rhabdomyolysis (release of AST, CRE, and myoglobin) and consequential kidney damage all caused by the applied essential oil of *M. officinalis*.

3.3.3. Histopathological findings

Total liver, kidney, stomach and duodenum injury scores, as well as partial scores relating to specific histomorphological changes caused by the treatment with *M. officinalis* essential oil are presented in Table 3. The dose increase resulted in the increase of the total tissue injury scores, while the control group of animals displayed low values of this score: 1.7, 0.25, 0 and 0.5 for liver, kidney, gastric and duodenal tissue, respectively (Table 3). The livers of mice that did not receive the

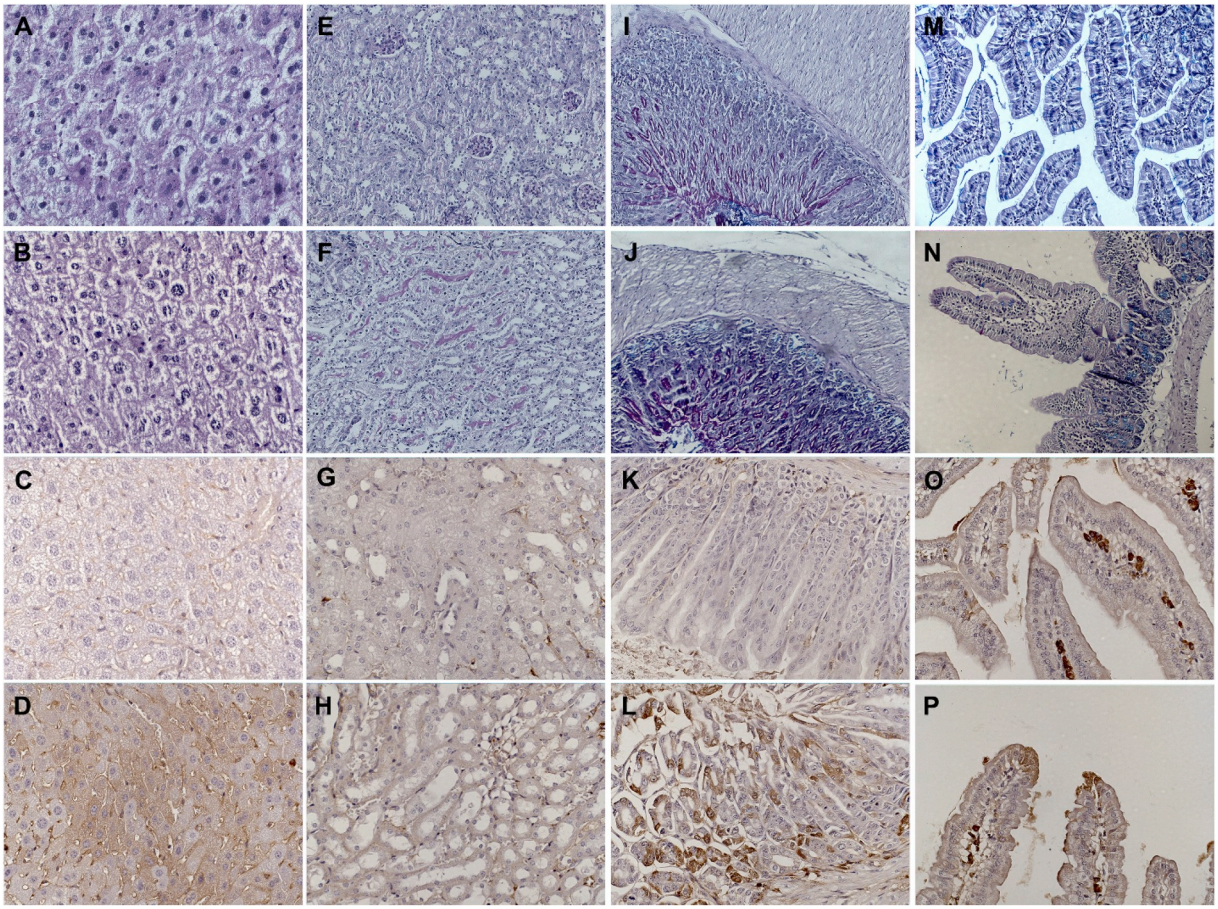

Fig. 5. Changes in liver (A–D), kidney (F–H), stomach (I–L) and duodenum (M–P) microscopic appearance after *Melissa officinalis* essential oil application stained with PAS and for 4-HNE presence. Normal glycogen (PAS-positive) present as granules in hepatocytes (A; x400); Glycogen depletion in hepatocytes (B; x400); Negative 4-HNE immunostaining in control group liver tissue (C; x400); Areas of 4-HNE positive hepatocytes overlapping with areas of hepatocytes with hypereosinophilic cytoplasm (D; x400). Kidney structures from untreated animals with occasional PAS positivity in tubule lumens belonging probably to tubular brush border (E; x200); Significant amounts of PAS-positive tubular casts mainly (F, x200); normal-appearing kidney structures with no 4-HNE immunopositive cells (G; x400); 4-HNE immunopositivity in occasional proximal and distal tubules (H, x400). Stomach glandular portion with normal PAS and AB positive glycoprotein amounts (I; x200); glandular mucosa of animals treated with essential oil showing increased amounts of PAS and AB positive glycoproteins (J; x200); Gastric 4-HNE immunopositivity benign completely absent in control group animals and those treated with lower doses of essential oil (K; x400) and significantly increased in those treated with higher doses (L; x400). Decrease in duodenal AB-positive glycoprotein amounts, compared to the control group (M; x200), was seen in animals treated with essential oil (N; x200); 4-HNE positivity in the control group of animals was only occasionally present in submucosa or muscular layer (O; x200); different doses of the essential oil caused villi tip necrosis which presented itself as brown colored villi tips (P; x200).

essential oil had characteristic lobular architecture and obvious sinusoids, well defined and normal appearing cell structures, with clear central vein and portal spaces (Fig. 4A). Liver tissue changes observed after animal exposure to high doses of the essential oil were predominantly found in zones I and II of the liver lobule (Fig. 4B), while in some cases all three zones were affected (mostly for higher doses). This zonal distribution is somewhat expected since the blood from the gastrointestinal tract, that carries the potentially toxic substances, is transported to the liver through the hepatic portal vein to the portal area (McQueen, 2010). Thus, the cells from zones I and II of the liver lobule are the first to suffer the damage caused by the intoxicant, i.e. the essential oil, where different degrees of hepatocyte degeneration in the form of microvesicular cytoplasmic inclusions and parenchymatous degeneration (Table 3 and Fig. 4B) were found. Besides being most affected by the specific blood supply, these hepatic cells might be suffering from a specific effect of the essential-oil constituents. CYP-enzymes located in these cells play a significant role in liver tissue damage (McQueen, 2010), and since a number of constituents are known to inhibit such enzymes, an impairment of the enzyme activities is possible. The detected hepatocyte 4-HNE positivity distribution mainly followed the same zonal distribution as hepatocyte degeneration observed (Fig. 5C and D).

The change in the number of polymorphonuclear eosinophilic leukocytes or macrophages surrounding the central vein or portal spaces that was detected (Table 3) could not be correlated with the applied dose of the essential oil. On the other hand, the degree of vascular congestion, present primarily in the liver central veins and in the portal spaces blood vessels, and sinus narrowing, partially correlates with the applied dose of the oil. Hepatocytes with karyopyknosis could be seen throughout the liver tissue in the treated animals, being most frequent in zone I and near the areas with hepatocytes with hypereosinophilic cytoplasm (Table 3 and Fig. 4C). The eosinophilic cytoplasm in certain hepatocytes might be the consequence of cell organelle swelling and lysosome rupture, being the initial step in hepatocytes necrosis (Pandey et al., 2008). However, the actual signs of necrosis have not been seen in mice livers. Interestingly, in the liver of rats treated with *C. citratus* essential oil (sharing a similar chemical composition with *M. officinalis*), hepatocyte necrosis and numerous leukocyte forming granuloma were detected (Fandohan et al., 2008). At a certain degree, 4-HNE positivity overlapped with the areas of hepatocytes with a hypereosinophilic cytoplasm (Figs. 4C and 5D). The liver tissue of mice from the control group showed high PAS-staining intensity (a significant amount of

glycogen) in all hepatocytes (Fig. 5A), while the animals treated with increasing doses of the essential oil displayed reduced glycogen distribution in zone III (scores between 0.7 and 1.2; Fig. 5B).

Light microscopy evaluation of kidney sections from the untreated animals showed the normal morphology of renal parenchyma, both cortex, and medulla, with well-defined tubules and glomeruli (Fig. 4D). In the renal cortex, its inner parts, of mice exposed to increasing doses of the essential oil, different degrees of glomerular hypertrophy (reduction of urinary spaces), tubular cell vacuolization (relatively rare with scores below 1.0) and degeneration (cloudy swelling), with occasional tubular atrophy could be seen (Table 3 and Fig. 4E). The analysis of immunohistochemically stained kidney tissue for 4-HNE revealed the presence of this lipid-peroxidation marker mainly in cells belonging to the parietal layer of Bowman's spaces and Henle's loop, and occasionally in proximal and distal tubules (Fig. 5H), while the control group tissues showed no immunopositivity (Fig. 5G). The areas of proximal/distal tubular edema (scores between 1.0 and 2.25) displayed narrow lumens and took star shape; occasional loss of microvillus in the proximal tubules could also be seen (Figs. 4F and 5F). These tubule-related changes could be contributed to the increased concentration of the potentially toxic essential-oil constituents in the urinary filtrate (McQueen, 2010). A certain degree of capillary dilation and blood stasis (predominantly in the medulla), seen in the liver tissue as well, and mononuclear cell infiltration around tubules and/or blood vessels (Fig. 4E), were detected. Renal pyramids and medullary structures retained normal appearance in all experimental groups.

Tubular brush border integrity could be related to GSH content in the kidney tissue, since the γ-GT localized in brush border plays an important role in GSH maintenance (Lee et al., 2004). The loss of tubular brush border could occasionally be seen on PAS-stained kidney sections (Fig. 5E and F), especially in groups treated with higher doses of the essential oil. The potential rhabdomyolysis occurring after the application of the essential oil could contribute to the kidney damage, as well. This fact can be further supported by the presence of tubular casts observed on kidney sections, from mice treated with all doses of *M. officinalis* essential oil, found on both HE- and PAS-stained (Table 3, Figs. 4F and 5F) kidney-tissue sections. These casts could originate from Tamm–Horsfall protein–myoglobin complex precipitation in the renal tubules with the addition of destroyed tubule cells (Bosch and Poch, 2009). It is evident that with the increase in the essential-oil dose, the amount of PAS-positive tubular casts increases (Table 3), which correlates well with the increase in AST and CRE serum levels (Table 2).

Normal glandular architecture, free from any pathological changes, of both gastric and duodenal tissues, was observed in the control group of animals (Fig. 4G and Table 3). Gastric mucosa appeared as the innermost lining of the stomach wall, being the largest and widest portion of the wall, while its majority was comprised of simple tubular gastric glands opening singly or in a group. The muscular layer was covered by serosa, submucosa, and mucosa and no inflammatory cell infiltration was present (Fig. 4G). The gastric tissue sections obtained from the animals treated with increasing doses of the essential oil displayed inflammatory cells presence in the submucosa/*lamina propria*, especially in the cardiac and antropyloric portions of the stomach (Table 3). The intensity of inflammation varied with the applied dose of the essential oil, being almost absent in some cases, while in others the intensity could be considered severe (Fig. 4H). Similar pathological changes, inflammatory leukocytes in the *lamina propria* and mucosal atrophy, were detected in rats treated with *C. citratus* essential oil (Fandohan et al., 2008). Occasionally, vacuolization in some gastric glands, with score values not above 0.5, could be seen (Table 3). Also, in the deeper layers of the stomach wall, the submucosa, capillary dilation, and edema could be seen occasionally (Fig. 4I). In the gastric tissue of mice treated with the essential oil, 4-HNE positivity varied with the applied dose of the essential oil; being completely absent (score 0.0) in the animals treated with the lower doses and significantly increased (score 2.0) in those treated with the higher ones (Table 3). This 4-HNE positivity was present mainly in the gastric glandular tissue, the mucosa, of the pyloric part of the stomach (Fig. 5K and L), but in cases where the higher doses were administered the complete gastric mucosa was affected.

Duodenal mucosa in the control group animals appeared as the deepest layer of the duodenum wall with normal long, finger-like, and slender villi arrangement. The villous epithelium was undamaged and had a regular thickness, with occasional inflammatory cell present within the stroma (Fig. 4J). Crypt length and enterocyte proliferation appeared normal as well. Characteristic Brunner's glands started to appear from the transitional zone between the gastric and duodenal mucosa and extend into the duodenal submucosa. In the submucosal layer, no vascular congestion, inflammatory cell infiltration or lymphatic dilatation was found (Fig. 4J). Immunohistochemical staining for 4-HNE in the duodenal tissue of the control animals appeared negative, where only occasional cells from the submucosa or muscular layer were positively colored in brown (Fig. 5O). In the treated animals dose-dependent changes (according to the pathological score obtained) in duodenal mucosa appearance could be seen (Fig. 4L and Table 3). The main pathological findings include: villi tip necrosis, especially in the animals that received high doses of the essential oil, and inflammatory cell infiltrate (Fig. 4K and L). These changes, found on duodenal villi, are somewhat expected since the small intestine is the place where the absorption of toxicants occurs due to the relatively large surface area and longer contact time (McQueen, 2010). Immunohistochemical staining of the duodenal tissue with the 4-HNE antibody confirmed the pathological findings (Figs. 4L and 5P), where a significant number of brown-colored villi tips was found in the animal groups that received 2 and 3 g kg^{-1} of the essential oil (Fig. 5P and Table 3). The animals that received lower doses of the essential oil, only an occasional enterocyte appeared to be positive to 4-HNE staining.

Histochemical AB/PAS technique was used for the semiquantitative determination of neutral (PAS-positive) and acidic (AB-positive) glycoproteins present in the gastric and duodenal tissues of the animals treated with *M. officinalis* essential oil. In the stomachs of the control group of animals, PAS-positive mucus was predominantly located on the gastric mucosal surface, while AB-positive mucus could be found in deeper layers of the pyloric mucosa (Fig. 5I). The duodenum of untreated animals showed only AB-positive mucus production, in the villi goblet and Bruner cells, as well as in the crypt gland cells (Fig. 5M). The application of the essential oil did not alter the distribution patterns of the mucus but increased the production of both PAS- and AB-positive mucus in the stomach/duodenum (Fig. 5J and N, Table 3). The mucus production throughout the gastrointestinal system, particularly PAS-positive, is known to contribute to the mucosal protection and its integrity preservation, especially in the upper parts (i.e. the stomach) (Slomiany et al., 1987). Thus, the increased production of PAS-positive mucus could be the consequence of the essential-oil stimulating effects, as well as the response of the animal organism to toxic substances present in the gastrointestinal system.

3.3.4. Tissue damage biochemical parameters

Based on the obtained results of different biochemical parameters reflecting tissue damage, measured in tissue homogenates, one can say that the applied essential oil caused tissue damage in rather an unspecific manner. Some of the evaluated parameters appeared to be above/below the upper/lower C.I. value (Table 4) suggesting a more or less pronounced damaging effect of the applied oil.

The nitrite levels in the tissue homogenates were not altered by the lower doses of the essential oil (or the SDs were large), however, the two highest doses caused an increase in tissue NO-levels above the upper C.I. value (Table 4). Besides the inflammatory cells, NO can be generated by other cells such as vascular smooth muscle cells, medullary interstitial and mesangial cells of the kidneys (Rolle et al., 2002) and by hepatocytes and Ito cells in the liver (Hon et al., 2002). These results could be brought into connection with the occurrence of

Table 4
Estimated liver and kidney tissues homogenate parameters related to tissue damage.

Dose (g kg^{-1}) and target tissue/Tissue damage-related parameter		MDA (nmol g^{-1} tissue)	CAT (IU L^{-1})	NO_2^- (μmol L^{-1})	MPO (O.D. x 1000)	GSH (μmol g^{-1} tissue)
1	Liver	66.4 ± 7.7	63.5 ± 35.1	20.1 ± 15.3	260.1 ± 63.6	3.15 ± 0.20
	Kidney	30.5 ± 2.8	145.2 ± 16.2	5.9 ± 3.2	112.5 ± 17.7	5.19 ± 0.16
1.25	Liver	88.7 ± 29.1	82.3 ± 21.5	12.1 ± 4.0	204.0 ± 15.6	2.68 ± 0.19
	Kidney	35.1 ± 3.6	153.5 ± 12.7	4.9 ± 1.7	125.0 ± 36.8	2.78 ± 1.60
1.5	Liver	57.8 ± 0.2	95.5 ± 12.5	8.2 ± 0.7	164.5 ± 41.7	2.74 ± 0.32
	Kidney	36.6 ± 4.7	109.6 ± 19.5	5.3 ± 1.6	141.7 ± 24.7	2.91 ± 0.45
2	Liver	74.6 ± 5.8	57.6 ± 25.8	9.9 ± 1.7	172.0 ± 28.3	2.24 ± 0.46
	Kidney	35.5 ± 13.9	78.7 ± 9.5	5.7 ± 1.3	206.0 ± 78.8	2.56 ± 0.37
3	Liver	133.4 ± 26.0	82.3 ± 3.5	10.5 ± 0.7	209.5 ± 14.1	2.15 ± 0.12
	Kidney	40.9 ± 2.1	92.5 ± 4.7	7.7 ± 1.0	316.5 ± 26.2	2.7 ± 0.19
Vehicle (10 mL kg^{-1})	Liver	47.9 ± 5.8	120.5 ± 15.7	7.19 ± 3.86	202.5 ± 23.3	3.38 ± 0.45
	Kidney	19.5 ± 5.6	147 ± 25	3.76 ± 1.73	98.5 ± 10.1	5.35 ± 0.35
C.I. 95%	Liver	51.9–48.9	145.2–95.8	9.82–4.56	218.7–186.3	3.69–3.07
	Kidney	23.4–15.6	165.1–130.5	4.96–2.57	105.4–91.5	5.60–5.11

Data are given as the mean values ± SD.

perivascular and/or peritubular inflammatory cell infiltration in the kidneys (Fig. 4F and Table 3), which might be responsible for the increase in NO-generation and tissue nitrosative damage occurring in the kidney/liver. Generated NO reacts with reactive oxygen species (ROS) forming reactive nitrogen species that are known to cause GSH tissue depletion, oxidation of fatty acids, etc. (Iwakiri and Kim, 2015). Also, NO and related ROS products inducing GSH depletion reflect the liver's ability to detoxify the essential-oil components allowing them to possibly interact with different cell proteins (Iwakiri and Kim, 2015).

The activity of MPO determined in the liver tissue of animals treated with different doses of the essential oil was generally within the C.I. values (Table 4). However, almost all doses of the essential oil increased the activity of MPO in the renal tissue of the exposed mice (Table 4). MPO activity represents a sensitive marker of polymorphonuclear cell infiltration, which is evident in the kidney tissue of animals exposed to the essential oil. The generated products of MPO, chlorinating oxidants coming from chlorides and H_2O_2, are able to cause cell damage by reacting with amino acids, proteins, carbohydrates, lipids, and nucleobases. One may say that the activity of MPO is in a good correlation with the cell lipid damage (Kolli et al., 2009). One of the most important lipid-peroxidation products is 4-HNE, which is involved in the modulation of a number of signaling processes predominantly by the formation of covalent adducts with nucleophilic functional groups in proteins, nucleic acids, and membrane lipids (Zhong and Yin, 2015). This increase in kidney homogenate MPO activity was followed by a moderate increase in 4-HNE immunohistochemical positivity (Tables 3 and 4) in the kidneys of animals treated with high doses of the essential oil (Fig. 5H).

Catalase (CAT) is considered to be one of the key enzymes that significantly contributes to the reduction of ROS by scavenging H_2O_2 in cells. The results of the present study demonstrate a significant decrease in the liver and kidney CAT activity, below lower C.I. value, after a single application of *M. officinalis* essential oil (Table 4). The decrease in the tissue CAT activity could be contributed to several factors: (i) a direct inhibitory action of the essential-oil constituents on the enzyme activity/protein expression; (ii) an increase in H_2O_2 can cause both inactivation and/or consumption of CAT in the tissues (Ahmed et al., 2015); (iii) a tissue NO-increase can lead to the degradation of the enzyme (Brown, 1995). All of the possible mechanisms that could alter CAT activity could impair the tissue's ability to prevent ROS mediated damage.

Malondialdehyde, one of the main products of lipid-peroxidation in addition to 4-HNE, was found to be increased in both the liver and kidney tissues of mice exposed to high doses of the essential oil (Table 4). Apart from 4-HNE, MDA reflects the lipid peroxidation tissue damage caused by the potentially toxic essential-oil components, as well. These products of lipid peroxidation formed, originating from ROS - partially generated by MPO and/or persisting due to the decrease in CAT activity, could lead to cell membrane damage that is followed by a serious cell function impairment (Kolli et al., 2009). Changes occurring in cell functioning primarily involve fluidity and selective permeability of membranes and signal transduction (Halliwell and Gutteridge, 1984). The measured MDA amounts in the liver/kidney tissue are in accordance with 4-HNE immunopositivity found on the liver and kidney tissue sections of the same animals (Table 3 and Fig. 5D and H), where the highest dose of the essential oil produced the most significant increase in MDA levels and 4-HNE score in the liver tissue (Tables 3 and 4). Although the increase in kidney MDA is almost double in value compared to the vehicle-treated group, the 4-HNE score does not follow this increase (Tables 3 and 4). This discrepancy in kidney MDA amounts and 4-HNE expression could possibly be the consequence of tissue-specific reactions to the applied essential oil, or a reaction of the aldehydic components (citronellal, neral or geranial) from the essential oil itself giving an increased false-positive reaction. The difference in the lipid peroxidation products (MDA and 4-HNE) abundance was previously found in the serum of patients with a stroke, where 4-HNE was suggested to be a better biomarker for stroke (Guo et al., 2013).

The amount of GSH, the most abundant low molecular weight thiol, which reflects tissue redox status, in the livers and kidney of animals treated with the essential oil was reduced below the lower C.I. value (Table 4). This difference was more pronounced in the kidney tissue, where certain doses decreased the levels of GSH by more than a half. Reduced glutathione represents one of the main non-enzymatic tissue defense cascades against oxidative injury and the diminution of GSH amount in liver and kidney tissues correlates accordingly with the increase in tissue MDA concentration and a decrease in CAT activity (Table 4). Additionally, the observed GSH decrease is in a good correlation with the increase in serum γ-GT (Table 2), which is responsible for maintaining the tissue glutathione homeostasis and its extracellular degradation (Lee et al., 2004). Partially preserved brush border in the proximal tubules of animals treated with the essential oil (found in the PAS-stained kidney tissue, Fig. 5F) might also explain the found GSH levels. Namely, the γ-GT localized on the luminal surface kidney brush border membrane (Hahn and Oberrauch, 1978) hydrolyzes GSH, thus its absence leads to a decrease in amino acids needed for GSH synthesis.

4. Conclusions

GC-MS and GC-FID analyses of the herein tested *M. officinalis* essential-oil samples, isolated from the aerial parts, permitted the identification of 133 essential-oil constituents, among them, 26 compounds are reported here for the first time as constituents of *M. officinalis*

essential oil.

The oral application of *M. officinalis* essential oil to mice produced significant changes in animal behavior, as well as in the biochemical parameters reflecting liver and kidney functions. When doses higher than 1 g kg^{-1} were orally administered, different pathological changes in the stomach, duodenum, liver, and kidneys were detected. Additionally, *M. officinalis* essential oil produced the depletion of liver/kidney antioxidant capacities and increased the rate of lipid peroxidation. The determined LD_{50} in BALB/c mice was 2.57 g kg^{-1} and the essential oil can be considered as only moderately toxic and could be used by humans. Although previous evaluation of *M. officinalis* essential oil acute toxicity in mice suggested that its LD_{50} value lays above 2 g, kg^{-1}, that study reported that there were no significant changes in animal behavior, general appearance or any signs of toxicity after a 2 g kg^{-1} application (Bounihi et al., 2014). In a previous sub-acute toxicity model in rats, similar to our results, *M. officinalis* essential oil application produced mild kidney damage, observed both through an increase in blood urea levels and microscopic tissue damage in the form of glomerular ischemic lesions and minimal focal tubular necrosis.

Declaration of competing interest

The authors declare that they have no known competing financial interests or personal relationships that could have appeared to influence the work reported in this paper.

Acknowledgment

This publication is a part of Nikola M. Stojanović's Ph.D. thesis, under the supervision of Pavle J. Randjelović. This work was supported by the Ministry of Education, Science and Technological Development of Serbia (Project No. 172061).

Appendix A. Supplementary data

Supplementary data to this article can be found online at https://doi.org/10.1016/j.fct.2019.110794.

Transparency document

Transparency document related to this article can be found online at https://doi.org/10.1016/j.fct.2019.110794.

References

Abudayyak, M., Nath, E.Ö., Özhan, G., 2015. Toxic potentials of ten herbs commonly used for aphrodisiac effect in Turkey. Turk. J. Med. Sci. 45, 496–506.
Ahmed, W., Zaki, A., Nabil, T., 2015. Prevention of methotrexate-induced nephrotoxicity by concomitant administration of garlic aqueous extract in rat. Turk. J. Med. Sci. 45, 507–516.
Ballard, C.G., O'Brien, J.T., Reichelt, K., Perry, E.K., 2002. Aromatherapy as a safe and effective treatment for the management of agitation in severe dementia: the results of a double-blind, placebo-controlled trial with *Melissa*. J. Clin. Psychiatry 63, 553–558.
Barnes, J., Anderson, L., Phillipson, J.D., 2002. Herbal Medicines. A Guide for Healthcare Professionals, second ed. Pharmaceutical Press, London, Chicago, USA.
Basta, A., Tzakou, O., Couladis, M., 2005. Composition of the leaves essential oil of *Melissa officinalis* from Greece. Flavour Fragrance J. 20, 642–644.
Bayat, M., Tameh, A.A., Ghahremani, M.H., Akbari, M., Mehr, S.E., Khanavi, M., Hassanzadeh, G., 2012. Neuroprotective properties of *Melissa officinalis* after hypoxic-ischemic injury both in vitro and in vivo. DARU J. Pharmaceut. Sci. 20, 1–10.
Bosch, X., Poch, E., 2009. Rhabdomyolysis and acute kidney injury. N. Engl. J. Med. 361, 62–72.
Bounihi, A., Alnamer, R., Hajjaj, G., Cherrah, Y., Zellou, A., 2014. Investigation of essential oil of *Melissa officinalis* for acute and sub-chronic oral toxicity. Int. J. Pharm. 4, 40–46.
Brown, G.C., 1995. Reversible binding and inhibition of catalase by nitric oxide. Eur. J. Biochem. 232, 188–191.
Buege, J.A., Aust, S.D., 1978. Microsomal lipid peroxidation. Methods Enzymol. 52, 302–310.
Chizzolla, R., Lohwasser, U., Franz, C., 2018. Biodiversity within *Melissa officinalis*: variability of bioactive compounds in a cultivated collection. Molecules 23, 294.
Chung, M., Cho, S.Y., Bhuiya, M.J., Kim, K.H., Lee, S.J., 2010. Anti-diabetic effects of lemon balm (*Melissa officinalis)* essential oil on glucose-and lipid-regulating enzymes in type 2 diabetic mice. Br. J. Nutr. 104, 180–188.
ECHA http://echa.europa.eu/hr/registration-dossier/-/registered-dossier/11672/7/3/5 - website, Accessed date: 4 August 2019.
Ellman, G., 1959. Tissue sulfhydryl groups. Arch. Biochem. Biophys. 82, 70–77.
ESCOP, 2003. Monographs, second ed. European Scientific Cooperative on Phytotherapy, Exeter.
Fandohan, P., Gnonlonfin, B., Laleye, A., Gbenou, J.D., Darboux, R., Moudachirou, M., 2008. Toxicity and gastric tolerance of essential oils from *Cymbopogon citratus, Ocimum gratissimum* and *Ocimum basilicum* in Wistar rats. Food Chem. Toxicol. 46, 2493–2497.
Goth, L., 1991. A simple method for determination of serum catalase activity and revision of reference range. Clin. Chim. Acta 196, 143–151.
Guo, J.M., Liu, A.J., Zang, P., Dong, W.Z., Ying, L., Wang, W., Xu, P., Song, X.R., Cai, J., Zhang, S.Q., Duan, J.L., Mehta, J.L., Su, D.F., 2013. ALDH2 protects against stroke by clearing 4-HNE. Cell Res. 23, 915–930.
Hahn, R., Oberrauch, W., 1978. Unidirectional transport of reduced glutathione in rat liver and its metabolization in the extracellular space. In: Sies, H., Wendel, A. (Eds.), Functions of Glutathione in Liver and Kidney, pp. 32–40.
Halliwell, B., Gutteridge, J., 1984. Lipid peroxidation, oxygen radicals, cell damage, and antioxidant therapy. Lancet 23, 1396–1398.
Hassanzadeh, G., Pasbakhsh, P., Akbari, M., Shokri, S., Ghahremani, M., Amin, G., Kashani, I., Tameh, A.A., 2011. Neuroprotective properties of *Melissa officinalis* l. extract against ecstasy-induced neurotoxicity. Cell J. (Yakhteh) 13, 25–30.
Hon, W.M., Lee, K.H., Khoo, H.E., 2002. Nitric oxide in liver diseases, friend, foe, or just passerby? Ann. N. Y. Acad. Sci. 962, 275–295.
Iwakiri, Y., Kim, M.Y., 2015. Nitric oxide in liver diseases. Trends Pharmacol. Sci. 36, 524–536.
Johnston, D.E., 1999. Special considerations in interpreting liver function tests. Am. Fam. Physician 84, 2223–2230.
Keltz, E., Khan, Y.F., Man, G., 2013. Rhabdomyolysis. The role of diagnostic and prognostic factors. Muscles Ligaments Tendons J. 3, 303–312.
Kolli, V.K., Abraham, P., Isaac, B., Selvakumar, D., 2009. Neutrophil infiltration and oxidative stress may play a critical role in methotrexate-induced renal damage. Chemotherapy 55, 83–90.
Lee, D.H., Blomhoff, R., Jacobs Jr., D.R., 2004. Is serum gamma glutamyltransferase a marker of oxidative stress? Free Radic. Res. 38, 535–539.
Lenaerts, A.J., Johnson, C.M., Marrieta, K.S., Gruppo, V., Orme, I.M., 2005. Significant increases in the levels of liver enzymes in mice treated with anti-tuberculosis drugs. Int. J. Antimicrob. Agents 26, 152–158.
Lin, J., Wang, C., 1986. Protection of crocin dyes in the acute hepatic damage induced by aflatoxin B and dimethylnitrosamine in rats. Carcinogenesis 7, 595–599.
McQueen, C., 2010. Comprehensive Toxicology, second ed. Elsevier Science & Technology, Oxford, UK.
Nurzyńska-Wierdak, R., Bogucka-Kocka, A., Szymczak, G., 2014. Volatile constituents of *Melissa officinalis* leaves determined by plant age. Nat. Prod. Commun. 9, 703–706.
Olivero-Verbel, J., González-Cervera, T., Güette-Fernandez, J., Jaramillo-Colorado, B., Stashenko, E., 2010. Chemical composition and antioxidant activity of essential oils isolated from Colombian plants. Rev. Bras. Pharmacogn. 20, 568–574.
Pandey, G., Srivastava, D.N., Madhuri, S., 2008. A standard hepatotoxic model produced by paracetamol in rat. Toxicol. Int. 15, 69–70.
Patora, J., Majda, T., Gora, J., Klimek, B., 2003. Variability in the content and composition of essential oil from lemon balm (*Melissa officinalis* L.) cultivated in Poland. Acta Pol. Pharm. 60, 395–400.
Radulović, N.S., Dekić, M.S., Ranđelović, P.J., Stojanović, N.M., Zarubica, A.R., Stojanović-Radić, Z.Z., 2012. Toxic essential oils: anxiolytic, antinociceptive and antimicrobial properties of the yarrow *Achillea umbellata* Sibth. et Sm. (Asteraceae) volatiles. Food Chem. Toxicol. 50, 2016–2026.
Radulović, N.S., Filipović, S.I., Zlatković, D.B., Djordjević, M.R., Stojanović, N.M., Randjelović, P.J., Mitić, K.V., Jevtović-Stoimenov, T., Randjelović, V.N., 2016. Immunomodulatory pinguisane-type sesquiterpenes from the liverwort *Porella cordaeana* (Porellaceae): the "new old" furanopinguisanol and its oxidation product exert mutually different effects on rat splenocytes. RSC Adv. 6, 41847–41860.
Radulović, N.S., Genčić, M., Stojanović, N.M., Randjelović, P.J., Stojanović-Radić, Z.Z., Stojiljković, N., 2017. Toxic essential oils. Part V: behaviour modulating and toxic properties of thujones and thujone-containing essential oils of *Salvia officinalis* L., *Artemisia absinthium* L., *Thuja occidentalis* L. and *Tanacetum vulgare* L. Food Chem. Toxicol. 105, 355–369.
Radulović, N.S., Jovanović, I., Ilić, I.R., Randjelović, P.J., Stojanović, N.M., Miltojević, A.B., 2013c. Methyl and isopropyl N-methylanthranilates attenuate diclofenac- and ethanol-induced gastric lesions in rats. Life Sci. 93, 840–846.
Radulović, N.S., Mladenović, M.Z., Blagojević, P.D., Stojanović-Radić, Z.Z., Ilic-Tomic, T., Senerovic, L., Nikodinovic-Runic, J., 2013b. Toxic essential oils. Part III: identification and biological activity of new allylmethoxyphenyl esters from a Chamomile species (*Anthemis segetalis* Ten.). Food Chem. Toxicol. 62, 554–565.
Radulović, N.S., Mladenović, M.Z., Randjelović, P.J., Stojanović, N.M., Dekić, M.S., Blagojević, P.D., 2015a. Toxic essential oils. Part IV: the essential oil of *Achillea falcata* L. as a source of biologically/pharmacologically active *trans*-sabinyl esters. Food Chem. Toxicol. 80, 114–129.
Radulović, N.S., Ranđelović, P.J., Stojanović, N.M., Blagojević, P.D., Stojanović-Radić, Z.Z., Ilić, I.R., Đorđević, V.B., 2013a. Toxic essential oils. Part II: chemical, toxicological, pharmacological and microbiological profiles of *Artemisia annua* L. volatiles. Food Chem. Toxicol. 58, 37–49.
Radulović, N.S., Randjelović, P.J., Stojanović, N.M., Cakić, N.D., Bogdanović, G.A., Zivanović, A.V., 2015b. Aboriginal bush foods: a major phloroglucinol from Crimson Bottlebrush flowers (*Callistemon citrinus*, Myrtaceae) displays strong antinociceptive

and antiinflammatory activity. Food Res. Int. 77, 280–289.
Radulović, N.S., Zlatković, D.B., Mitić, K.V., Randjelović, P.J., Stojanović, N.M., 2014. Synthesis, spectral characterization, cytotoxicity and enzyme-inhibiting activity of new ferrocene–indole hybrids. Polyhedron 80, 134–141.
Rolle, U., Shima, H., Puri, P., 2002. Nitric oxide, enhanced by macrophage-colony stimulating factor, mediates renal damage in reflux nephropathy. Kidney Int. 62, 507–513.
Shakeri, A., Sahebkar, A., Javadi, B., 2016. *Melissa officinalis* L. – a review of its traditional uses, phytochemistry and pharmacology. J. Ethnopharmacol. 188, 204–228.
Sharopov, F.S., Wink, M., Khalifaev, D.R., Zhang, H., Dosoky, N.S., Setzer, W.N., 2013. Composition and bioactivity of the essential oil of *Melissa officinalis* L. growing wild in Tajikistan. Int. J. Trad. Nat. Med. 2, 86–96.
Slomiany, B.L., Sarosiek, J., Slomiany, A., 1987. Gastric mucus and the mucosal barrier. Dig. Dis. 5, 125–145.
Stojanović, N.M., Samardzić, Lj, Ranđelović, P.J., Radulović, N.S., 2017. Prevalence of self-medication practice with herbal products among non-psychotic psychiatric patients from southeastern Serbia: a cross-sectional study. Saudi Pharm. J. 25, 884–890.
Thapa, B.R., Walia, A., 2007. Liver function tests and their interpretation. Indian J. Pediatr. 74, 663–671.
Tisserand, R., Young, R., 2014. Essential Oil Safety: A Guide for Health Care Professionals, second ed. Churchill Livingstone, London, UK.
Ulbricht, C., Brendler, T., Gruenwald, J., Kligler, B., Keifer, D., Abrams, T.R., Woods, J., Boon, H., Kirkwood, C.D., Hackman, D.A., Basch, E., Lafferty, H.J., 2005. Lemon balm (*Melissa officinalis* L.): an evidence-based systematic review by the natural standard Research collaboration. J. Herb. Pharmacother. 5, 71–114.
Van den Dool, H., Kratz, P.D., 1963. A generalization of the retention index system including linear temperature programmed gas-liquid partition chromatography. J. Chromatogr. 11, 463–471.
Verma, R.S., Padalia, R.C., Chauhan, A., 2015. Evaluation of essential oil quality of lemon balm (*Melissa officinalis* L.) grown in two locations of northern India. J. Essent. Oil Res. 27, 412–416.
Vogl, S., Picker, P., Mihaly-Bison, J., Fakhrudin, N., Atanasov, A.G., Heiss, E.H., Wawrosch, C., Reznicek, G., Dirsch, V.M., Saukel, J., Kopp, B., 2013. Ethnopharmacological *in vitro* studies on Austria's folk medicine–an unexplored lore *in vitro* anti-inflammatory activities of Austrian traditional herbal drugs. J. Ethnopharmacol. 149, 750–771.
Weibrecht, K., Dayno, M., Darling, C., Bird, S.B., 2010. Liver aminotransferases are elevated with rhabdomyolysis in the absence of significant liver injury. J. Med. Toxicol. 6, 294–300.
Zhong, H., Yin, H., 2015. Role of lipid peroxidation derived 4-hydroxynonenal (4-HNE) in cancer: focusing on mitochondria. Red. Biol. 4, 193–199.